Mon. Not. R. Astron. Soc. **368,** 1055–1072 (2006) doi:10.1111/j.1365-2966.2006.10192.x

On the force-free magnetosphere of an aligned rotator

A. N. Timokhin★
Sternberg Astronomical Institute, Universitetskij pr. 13, 119992 Mocsow, Russia

Accepted 2006 February 7. Received 2006 January 29; in original form 2005 November 26

ABSTRACT

We investigate in detail the properties of the stationary force-free magnetosphere of an aligned rotator assuming the last closed field line is lying in the equatorial plane at large distances from pulsar. The pulsar equation is solved numerically using a multigrid code with high numerical resolution, and physical properties of the magnetosphere are obtained with high accuracy. We found a set of solutions with different sizes of the closed magnetic field line zone and verify the applicability of the force-free approximation. We discuss the role of electron–positron cascades in supporting the force-free magnetosphere and argue that the closed field line zone should grow with time at a slower rate than the light cylinder. This yields a pulsar breaking index of less than 3. It is shown that models of an aligned rotator magnetosphere with a widely accepted configuration of the magnetic field, such as the one considered in this paper, have serious difficulties. We discuss the solutions of this problem and argue that in any case pulsar energy losses should evolve with time differently than is predicted by the magnetodipolar formula.

Key words: MHD – stars: magnetic fields – pulsars: general.

1 INTRODUCTION

Since the first works on pulsar magnetospheres, a stationary force-free magnetosphere of an aligned rotator has been considered as an underlying model for the real pulsar magnetosphere for more than 30 years. Despite its degenerated character (this 'pulsar' does not even pulse), it is believed to reproduce qualitatively all the main properties of the real pulsar magnetosphere. For the near-aligned pulsars it should even give an adequate detailed description. The structure of the force-free magnetosphere of an aligned rotator can be described by the solution of a single scalar non-linear partial differential equation (PDE), the so-called 'pulsar equation', derived by Michel (1973b), Scharlemann & Wagoner (1973) and Okamoto (1974). This is an equation for the flux of the poloidal magnetic field. All other physical quantities describing the magnetosphere are related to the flux function Ψ, the poloidal current J and the angular velocity of the rotation of the magnetosphere Ω by algebraic relations.

An analytical solution of this equation with non-zero poloidal current seems to exist only for the split-monopole configuration of the magnetic field (Michel 1991) and for a slightly perturbed split monopole (Beskin, Kuznetsova & Rafikov 1998). For the dipole magnetic field an analytical solution for the case of zero poloidal current has been found (Michel 1973a; Mestel & Wang 1979), but this solution is valid only inside the light cylinder (LC). There were several works dedicated to the solution of the linearized pulsar equation, where the poloidal current and angular velocity were assumed to be proportional to the magnetic flux function, which made the equation linear, but they did not lead to the construction of a consistent model of an aligned rotator magnetosphere (see e.g. Beskin, Gurevich & Istomin 1983; Lyubarskii 1990; Beskin & Malyshkin 1998).

The first attempt to solve the non-linearised pulsar equation numerically was made by Contopoulos, Kazanas & Fendt (1999, hereafter CKF). They have shown, for the first time, that there exists a *self-consistent* solution with dipole magnetic field geometry near the neutron star (NS) and magnetic field lines smoothly passing through the LC. In that work the position of the null point[1] was fixed at the LC and the questions about applicability of the force-free approximation have been not investigated. The energy losses of the aligned rotator for the CKF solution have been calculated by Gruzinov (2005). Goodwin et al. (2004) have studied this problem more deeply, namely they have searched for the solution of the pulsar equation when the position of the null point is not fixed at the LC, but lies at different positions inside the LC. For any position of the null point they obtained solutions that smoothly passed the LC, but like CKF they have not studied the physical properties of the obtained solutions (e.g. energy losses, applicability of the force-free approximations, etc.). Their model, however, seems to be artificial, because they assumed non-zero pressure in the closed field line zone, which implies continuous energy injection into the closed field line domain. Recently Contopoulos (2005) addressed the case where the plasma rotation frequency in the open field line domain

★E-mail: atim@sai.msu.ru

[1] The point where the last closed field line intersects the equatorial plane.

is different from the rotation frequency of the NS. It was shown that there exists a unique solution of the pulsar equation for an arbitrary plasma rotation frequency, although a rather simple case when the plasma rotation frequency is constant has been considered. The applicability of the force-free approximations in the magnetosphere of an aligned rotator was considered in Timokhin (2005) and Contopoulos (2005), though in the latter work only for the null point located at the LC.

Recently different approach to the pulsar magnetosphere modelling has been developed by Spitkovsky (2005), Komissarov (2006) and McKinney (2006). They perform *time-dependent* simulations of the pulsar magnetosphere. In Komissarov (2006) the aligned rotator magnetosphere was modelled using a full magnetohydrodynamic (MHD) code; in McKinney (2006) the same modelling was performed with force-free code. The code of Anatoly Spitkovsky allows a 3D time-dependent simulation of the magnetosphere of inclined rotator to be performed by solving equations of force-free MHD. In these simulations the *existence* of the stationary force-free magnetospheric configuration was rigorously proved for the first time. Although this approach presents a big step towards the modelling of the real pulsar magnetosphere, in this paper we argue that it has serous limitations, namely that the properties of cascades supplying particles in the magnetosphere are not incorporated in these simulations. As will be discussed later, cascades can set non-trivial boundary conditions on the current density in the magnetosphere. Its incorporation in time-dependent codes would require some effort.

In this work we investigate the stationary problem, solving the pulsar equation numerically with high numerical resolution. We assume zero pressure in the closed field line region (cold plasma). As in all the above-mentioned works on the numerical modelling of a stationary aligned rotator magnetosphere, we assume a topology with the current sheet in an open field line domain being in the equatorial plane, i.e. configuration with a Y null point – see Fig. 1. This type of magnetosphere topology had became de facto the 'standard model', so we study it in detail and analyse its properties regarding many aspects of electrodynamics. Smooth solutions are obtained for *any* position of the null point inside the LC. A high numerical resolution allows one to accurately incorporate the return current flowing along the separatrix (the last closed field line) into the numerical procedure. With the high resolution of the numerical method used it was possible to calculate accurately the physical properties of the solutions such as the Goldreich–Julian (GJ) charge density, the magnetic field, energy losses and pointing flux distribution etc., to check the applicability of the force-free approximation and to consider the compatibility of the model with models of electron–positron cascades.

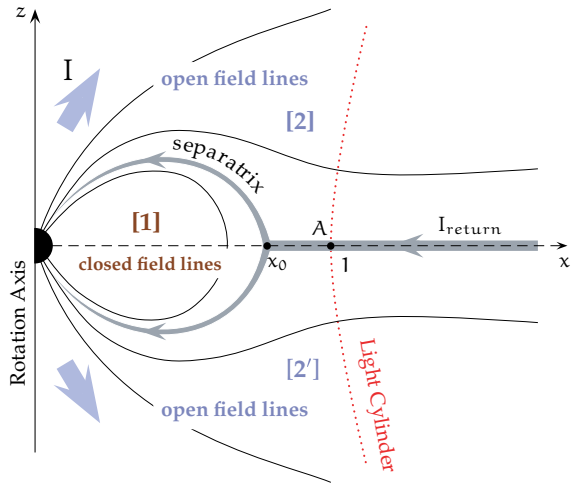

Figure 1. Configuration of the magnetic field in the magnetosphere of an aligned rotator with a Y null point – Y-configuration. After the null point x_0 the separatrix goes along the equatorial plane. The volume current I flows in the open field line zones [2] and [2′]. The current circuit closes somewhere beyond the LC. There could be a volume return current along some open field lines, but the largest part of it flows along the separatrix.

The adjustment of the current density in the polar cap cascade zone of the pulsar to the global magnetospheric structure was debated already in the first 10 years after the discovery of the pulsar (see e.g. Arons 1979). A concrete mechanism for the current density adjustment was proposed by Yu. Lyubarskij many years later, in 1992. At that time there was no self-consistent model of the pulsar magnetosphere and detailed discussion on this subject was difficult. Here we discuss the coupling between the polar cap cascade zone and the rest of the magnetosphere in the frame of the self-consistent model obtained in our simulations. We extend the picture proposed by Lyubarskij (1992) addressing the evolution of the current adjustment mechanism with ageing of the pulsar. We also prove the necessity of such a mechanism and discuss it in more detail in the frame of the cascade model proposed by Scharlemann, Arons & Fawley (1978). We underline the serious difficulties of a model with a Y null point regarding its compatibility with the space charge limited flow models of polar cap cascades and briefly discuss other possible magnetospheric configurations.

The plan of the paper is as follows. In Section, 2 important properties of the pulsar equation are discussed. The model used in the current work and numerical method are described in Section 3. Results of the numerical simulations are presented in Section 4. In Section 5 we discuss the role of polar cap cascades for the global structure of the magnetosphere, consider in detail the properties of the force-free magnetosphere with a Y null point, and highlight problems of the 'standard' model of an aligned rotator magnetosphere. A different topology of the magnetosphere, with an X null point, is briefly discussed at the end of the section. We summarize the most important results in Section 6.

2 THE PULSAR EQUATION

2.1 General equation

Here we adopt the widely used assumption that the *entire* magnetosphere of the NS is filled with plasma. In some works starved magnetosphere configurations have been debated (see e.g. Smith, Michel & Thacker 2001; Pétri, Heyvaerts & Bonazzola 2002), where there are several separated clouds of charged particles near the NS and no particle outflow, however there are indications that such a configuration is unstable against diocotron instability (Spitkovsky & Arons 2002; Spitkovsky 2004). Plasma in the magnetosphere has to be non-neutral in order to screen the longitudinal (directed along the magnetic field lines) component of the electric field, induced by the rotation of the NS. In the presence of the longitudinal electric field charged particles would be accelerated and their radiation will lead to copious electron–positron pair production in the super-strong magnetic field of a pulsar (Sturrock 1971), which finally results in the screening of the accelerating field.

The charge density necessary to cancel the longitudinal electric field, the so-called GJ charge density (Goldreich & Julian 1969), near the neutron star is given by

$$\rho_{\rm GJ} \simeq -\frac{\boldsymbol{\Omega}\cdot\boldsymbol{B}}{2\pi c}, \qquad (1)$$

where $\mathbf{\Omega}$ is angular velocity on neutron star rotation, $\boldsymbol{B}$ is magnetic field and c is the speed of light. Assuming that the NS has a dipolar magnetic field, the ratio of the particle kinetic energy density in the magnetosphere to the energy density of the magnetic field at the distance r can be estimated as

$$\frac{\varepsilon_{\rm kin}}{\varepsilon_B} \sim \frac{(\rho_{\rm GJ}/e)\, m_{\rm e}c^2\gamma}{(B^2/8\pi)} \simeq 1.4\times10^{-11}P^{-1}\left(\frac{\gamma}{10^7}\right)\left(\frac{B_0}{10^{12}\,{\rm G}}\right)^{-1}\left(\frac{r}{R_{\rm NS}}\right)^3, \quad (2)$$

where e and $m_{\rm e}$ are electron charge and mass respectively, $R_{\rm NS}$ is the neutron star radius, γ is the Lorentz factor of the accelerated particles, B_0 the magnetic field strength in Gauss near the magnetic poles of the star and P is the period of the pulsar rotation in seconds. All these quantities are normalized to their typical values in pulsars. This ratio is small (less than 1 per cent) in the region with a size of $\sim10^3\,P^{-1}$ radii of the neutron star. It could remain small at larger sizes, but here the magnetic field deviates substantially from the dipole field of the NS due to the currents flowing in the magnetosphere, and $\varepsilon_{\rm kin}/\varepsilon_B$ can be estimated only after a self-consistent solution for the structure of the magnetosphere is found. Thus, in the large domain surrounding the neutron star, we can use a force-free approximation when the particle inertia is neglected and the equation of motion takes the form

$$\rho\boldsymbol{E} + \frac{1}{c}[\boldsymbol{j}\times\boldsymbol{B}] = 0. \quad (3)$$

Hence, electric field $\boldsymbol{E}$ is perpendicular to the magnetic field $\boldsymbol{B}$. Charge density ρ and current density $\boldsymbol{j}$ in equation (3) can be found from the Maxwell equations (we consider a stationary problem):

$$\nabla\cdot\boldsymbol{E} = 4\pi\rho\,, \quad (4)$$

$$\nabla\times\boldsymbol{B} = \frac{4\pi}{c}\boldsymbol{j}\,, \quad (5)$$

With help of these equations, equation (3) can be written as

$$(\nabla\cdot\boldsymbol{E})\,\boldsymbol{E} + [\nabla\times\boldsymbol{B}]\times\boldsymbol{B} = 0\,. \quad (6)$$

In force-free electrodynamics (FFE)[2] the only possible motion of charged particles across magnetic field lines is the drift in crossed electrical and magnetic fields with the velocity

$$\boldsymbol{U}_{\rm D} = c\,\frac{\boldsymbol{E}\times\boldsymbol{B}}{B^2}\,. \quad (7)$$

Obviously $|\boldsymbol{U}_{\rm D}|$ must be less than c, or equivalently $|\boldsymbol{E}|$ must be less than $|\boldsymbol{B}|$. Generally speaking, equation (3) can have solutions where $|\boldsymbol{U}_{\rm D}| > c$. The surface, where $|\boldsymbol{U}_{\rm D}|$ reaches c, is commonly referred as the *light surface*. Beyond the light surface, where $|\boldsymbol{U}_{\rm D}| > c$, the force-free approximation cannot be applied. FFE is not self-consistent, because particle dynamics is ignored. Hence, each solution of equation (6) should be always checked for applicability of the force free approximation.

In the axisymmetric stationary case considered here, the magnetic field in cylindrical coordinates (ϖ, ϕ, Z) can be written as

$$\boldsymbol{B} = \frac{\nabla\Psi\times\boldsymbol{e}_\phi}{\varpi} + \frac{4\pi}{c}\frac{I}{\varpi}\boldsymbol{e}_\phi\,, \quad (8)$$

where $\boldsymbol{e}_\phi$ is the unit azimuthal, toroidal vector. In components

$$(B_\varpi, B_\phi, B_Z) = \left(-\frac{1}{\varpi}\partial_Z\Psi,\ \frac{4\pi}{c}\frac{I}{\varpi},\ \frac{1}{\varpi}\partial_\varpi\Psi\right)\,. \quad (9)$$

[2] Hereafter we use this shorter name for force-free degenerate electrodynamics (see e.g. Komissarov 2002; Blandford 2002, and references therein).

The scalar function Ψ is related to the magnetic flux $\Phi_{\rm mag}$ through a circle which has its centre at the point $(0, Z)$ and radius ϖ by $\Phi_{\rm mag} = 2\pi\Psi(\varpi, Z)$. Thus, lines of constant Ψ coincide with magnetic field lines. It could be easily verified that in the force-free case the scalar function $I(\varpi, Z)$ is constant along magnetic field lines, i.e

$$I \equiv I(\Psi)\,. \quad (10)$$

I is related to the total current J *outflowing* through the above mentioned circle by $J = 2\pi I(\varpi, Z)$.

In the quasi-stationary case the time derivative of $\boldsymbol{B}$ takes the form (see Mestel 1973)

$$\frac{\partial\boldsymbol{B}}{\partial t} = \nabla\times([\mathbf{\Omega}\times\boldsymbol{r}]\times\boldsymbol{B})\,. \quad (11)$$

Substituting this into the Faraday's law

$$\nabla\times\boldsymbol{E} = -\frac{1}{c}\partial_t\boldsymbol{B}\,, \quad (12)$$

we get for the electric field

$$\boldsymbol{E} = -\frac{\mathbf{\Omega}\times\boldsymbol{r}}{c}\times\boldsymbol{B} - \nabla V = -\frac{\Omega}{c}\nabla\Psi - \nabla V\,, \quad (13)$$

where V is the non-corotational (see below) part of the electric potential. The first term in (13) is poloidal and only the second term could make a contribution to the toroidal component. In the axisymmetric case $\partial_\phi V = 0$, and hence $\boldsymbol{E}$ is poloidal. In the force-free case $\boldsymbol{E}\perp\boldsymbol{B}$; from this it follows that $\boldsymbol{E}\cdot(\nabla\Psi\times\boldsymbol{e}_\phi) = 0$. Consequently, $\boldsymbol{E}\propto\nabla\Psi$ and we can write

$$\boldsymbol{E} = -\frac{\Omega_{\rm F}}{c}\nabla\Psi\,, \quad (14)$$

or in components

$$(E_\varpi, E_\phi, E_Z) = \left(-\frac{\Omega_{\rm F}}{c}\partial_\varpi\Psi,\ 0,\ -\frac{\Omega_{\rm F}}{c}\partial_Z\Psi\right)\,. \quad (15)$$

Substituting this expression together with equation (8) into the formula for the drift velocity (7), we get

$$\boldsymbol{U}_{\rm D} = \Omega_{\rm F}\varpi\boldsymbol{e}_\phi - \frac{4\pi}{c}\frac{I\Omega_{\rm F}}{B^2}\,\boldsymbol{B} \equiv \mathbf{\Omega}_{\rm F}\times\boldsymbol{r} - \kappa\boldsymbol{B}\,. \quad (16)$$

Thus the particle motion is composed from rotation with an angular velocity $\Omega_{\rm F}\equiv\Omega_{\rm F}\boldsymbol{e}_z$ and gliding along magnetic field lines. Hence, $\Omega_{\rm F}$ is the angular velocity of the rotation of the magnetic field lines. By substituting equation (14) into the stationary Faraday's law, one find $\nabla\Omega_{\rm F}\times\nabla\Psi = 0$. This implies that $\Omega_{\rm F}$ is constant along magnetic field lines:

$$\Omega_{\rm F} \equiv \Omega_{\rm F}(\Psi)\,. \quad (17)$$

Equation (17) is the well-known Ferraro isorotation law.

Finally, substituting $\boldsymbol{E}$ and $\boldsymbol{B}$ from equations (8) and (14) into equation (6) we get

$$\left(1-\frac{\Omega_{\rm F}^2\varpi^2}{c^2}\right)\nabla^2\Psi - \frac{2}{\varpi}\partial_\varpi\Psi + \left(\frac{4\pi}{c}\right)^2 I\frac{{\rm d}I}{d\Psi} - \frac{\varpi^2}{c^2}\Omega_{\rm F}\frac{d\Omega_{\rm F}}{d\Psi}(\nabla\Psi)^2 = 0 \quad (18)$$

This is the Grad–Shafranov equation for the poloidal magnetic field, the so-called pulsar equation, derived by Michel (1973b), Scharlemann & Wagoner (1973) and Okamoto (1974). This scalar PDE is of elliptical type. It is the poloidal part of the vector equation (6). The toroidal part of equation (6) is simply the relation (10). The pulsar equation has two integrals of motion – I and $\Omega_{\rm F}$. If we know them,

we can solve this equation for the function Ψ and determine the poloidal magnetic field. Electric and magnetic fields and all other parameters of the force-free magnetosphere can be found, because they are connected to Ψ, I and Ω_F by algebraic relations. In the frame of FFE, I and Ω_F are *free parameters*. They could be determined self-consistently in the full MHD, if electromagnetic cascades, setting boundary conditions, are also taken into account (see Beskin 2005). Nevertheless, one can get useful results in the force-free approximation. Equation (18) has one singular surface, the so-called *light cylinder*, where $\varpi = c/\Omega_F\,[\Psi(\varpi, Z)]$. As will be shown in the next subsection, the difference between Ω_F and Ω is small and the singular surface has a shape that is similar to a cylinder with the radius of $R_{LC} = c/\Omega$.

We normalize the variables ϖ and Z to R_{LC} and introduce new dimensionless coordinates $x \equiv \varpi/R_{LC}$ and $z \equiv Z/R_{LC}$. We will consider the case of dipolar magnetic field on the NS. Thus, near the star the magnetic field is given by

$$\Psi = \mu \frac{\varpi^2}{(\varpi^2 + Z^2)^{3/2}} \equiv \Psi_0 \frac{x^2}{(x^2 + z^2)^{3/2}}\,, \tag{19}$$

where $\mu = B_0 R_{NS}^3/2$ is the magnetic moment of the NS and $\Psi_0 \equiv \mu/R_{LC}$. We normalize Ψ to Ψ_0 and introduce the dimensionless function $\psi \equiv \Psi/\Psi_0$. Instead of the poloidal current function I we introduce a dimensionless function $S \equiv (4\pi/c)(R_{LC}/\Psi_0)I$. The angular velocity of the magnetic field line rotation is normalized to the angular velocity of the NS by the relation $\Omega_F(x, z) \equiv \beta(x, z)\,\Omega$. For these dimensionless functions the pulsar equation (18) takes the form

$$(\beta^2 x^2 - 1)(\partial_{xx}\psi + \partial_{zz}\psi) + \frac{\beta^2 x^2 + 1}{x}\partial_x\psi - S\frac{\mathrm{d}S}{\mathrm{d}\psi} + x^2\beta\frac{\mathrm{d}\beta}{\mathrm{d}\psi}(\nabla\psi)^2 = 0\,. \tag{20}$$

At the LC the coefficient found by second derivatives goes to zero and the pulsar equation has the form

$$2\beta\,\partial_x\psi = S\frac{\mathrm{d}S}{\mathrm{d}\psi} - \frac{1}{\beta}\frac{\mathrm{d}\beta}{\mathrm{d}\psi}(\nabla\psi)^2\,. \tag{21}$$

Let us now discuss the properties of the functions Ω_F and S.

2.2 Ω_F

From relation (17) it follows that V is constant along a magnetic field line. Hence, we could rewrite equation (13) in the form

$$\boldsymbol{E} = -\frac{1}{c}\left(\Omega + c\frac{\partial V}{\partial\Psi}\right)\nabla\Psi\,. \tag{22}$$

Comparing this expression with equation (14), we get

$$\Omega_F = \Omega + c\frac{\partial V}{\partial\Psi}\,. \tag{23}$$

If there were no potential difference between different magnetic field lines or between them and the surface of the pulsar, Ω_F would be equal to Ω. However, independently of the NS surface properties, a potential difference along open magnetic field lines will always be built up in the polar cap region of a pulsar (Ruderman & Sutherland 1975; Scharlemann et al. 1978; Muslimov & Tsygan 1992). This leads to the formation of a particle acceleration zone, where force-free approximation is not valid and charged particles are accelerated by the longitudinal electric field. Electron–positron pairs produced in the strong magnetic field of the pulsar by photons, emitted by accelerated particles, screen the accelerating field, and as the pair-production rate grows very rapidly with distance, the acceleration zone terminates in a rather thin layer called the pair-formation front (PFF). Above the PFF the accelerating field is screened, and FFE can be applied. The size of the acceleration zone is small compared to the overall size of the magnetosphere; its height varies from $\sim$100 m for young pulsars in models with no particle escape from the NS surface (Ruderman & Sutherland 1975) to 1–2 stellar radii in models where the particles freely escape the star surface (Scharlemann et al. 1978; Muslimov & Tsygan 1992). Geometrically, this small region could be neglected in the modelling of the global magnetospheric structure. The potential difference between the NS surface and the magnetic field lines should be taken into account by boundary conditions on V, which can be reformulated as boundary conditions on Ω_F. The potential difference along a magnetic field line in the acceleration zone is determined by the position of PFF, which depends on the local geometry of the magnetic field, close to the NS surface, and kinetic processes in the electron–positron cascade.

The relative difference of rotation velocities of plasma and NS can be estimated to an order of magnitude as

$$\frac{\delta\Omega}{\Omega} \equiv \frac{\Omega - \Omega_F}{\Omega} \simeq \frac{P}{2\pi}\frac{v_{rot}}{r_{pc}} \simeq 2.28\times10^{-11}\left(\frac{B_0}{10^{12}\,\mathrm{G}}\right)^{-1} P^2\Delta V\,, \tag{24}$$

where ΔV is the potential difference between the NS surface and the PFF (in statvolts), $r_{pc} \simeq \sqrt{R_{NS}^3\Omega/c}$ is the size of the polar cap, and $v_{rot} = c\Delta V/(B_0 r_{pc})$ is the linear velocity of the plasma rotation relative to the NS surface in the acceleration zone – see equation (31) in Ruderman & Sutherland (1975).

In the model with no particle escape from the NS surface, the potential difference is given by (Ruderman & Sutherland 1975, equation 23)

$$\Delta V \simeq 5.24\times10^9 P^{-1/7}\left(\frac{\rho_c}{10^6\,\mathrm{cm}}\right)^{4/7}\left(\frac{B_0}{10^{12}\,\mathrm{G}}\right)^{-1/7}, \tag{25}$$

where ρ_c is the curvature radius of the magnetic field lines. The potential difference is measured in statvolts. Substituting these expressions into equation (24) we get

$$\frac{\delta\Omega}{\Omega} \simeq 0.1\;P^{13/7}\left(\frac{\rho_c}{10^6\,\mathrm{cm}}\right)^{4/7}\left(\frac{B_0}{10^{12}\,\mathrm{G}}\right)^{-8/7}. \tag{26}$$

We see that, for relatively young pulsars with periods $P \lesssim 0.3$ s, this ratio is very small; $\sim$1 per cent. Even if the curvature radius of the field line is of the order of $\sim10^8$ cm (typical for a dipole magnetic field), for $P \lesssim 0.1$ s this ratio is $\sim$2 per cent.

For the model where particles freely escape the NS surface we use estimations from Hibschman & Arons (2001). The potential difference in the acceleration zone (Hibschman & Arons 2001, equations 17 and 18)

$$\Delta V^{h>r_{pc}} \simeq 9.87\times10^9 P^{-2}\left(\frac{B_0}{10^{12}\,\mathrm{G}}\right)h\,, \tag{27}$$

$$\Delta V^{h<r_{pc}} \simeq 1.11\times10^{12} P^{-3/2}\left(\frac{B_0}{10^{12}\,\mathrm{G}}\right)h^2\,. \tag{28}$$

Here h is the height of PFF above the NS surface in units of R_{NS}. The above estimations for accelerating potential are for the cases where $h > r_{pc}$ and $h < r_{pc}$, respectively. The potential differences are in statvolts. The heights of the PFF position due to photons emitted by

non-resonant inverse Compton scattering (NIC), curvature radiation (CR) and resonant inverse Compton scattering (RIC) of accelerated particles are given by

$$h_{\rm NIC} \simeq 0.40\, P \left(\frac{B_0}{10^{12}\,{\rm G}}\right)^{-1} T_6^{-2} f_\rho \tag{29}$$

$$h^{\rm c}_{\rm NIC} \simeq 0.12\, P^{1/4} \left(\frac{B_0}{10^{12}\,{\rm G}}\right)^{-1/2} T_6^{-1} f_\rho^{1/2} \tag{30}$$

$$h_{\rm CR} \simeq 0.68\, P^{19/12} \left(\frac{B_0}{10^{12}\,{\rm G}}\right)^{-5/6} f_\rho^{1/2} \tag{31}$$

$$h_{\rm RIC} \simeq 12 \left(\frac{B_0}{10^{12}\,{\rm G}}\right)^{-7/3} T_6^{-2/3} f_\rho\,, \tag{32}$$

see Hibschman & Arons (2001), equations (34), (32), (42) and (37) correspondingly. Label 'c' corresponds to the model where the NS surface is colder than the polar cap of the pulsar, heated by the return current. T_6 is the temperature of the polar cap in units of 10^6 K. The radius of curvature of the magnetic field lines is a factor f_ρ times the radius of curvature of a dipole field, i.e. $f_\rho \equiv \rho_c/\rho_c^{\rm dip} = P^{-1/2}\,\rho_c/(9.2\times10^7$ cm).

According to Hibschman & Arons (2001), in most pulsars the PFF height is set by NIC photons. In high-voltage pulsars, ones with the shortest periods (i.e. millisecond and youngest pulsars with $P \lesssim 0.3$ s), the PFF is set by the curvature photons. In both of these cases the resulting height of the PFF is larger than the size of the polar cap, $h > r_{\rm pc}$. RIC is important only for high field pulsars, with $B \gtrsim 1.2\times10^{13}$ G, in this case $h \ll r_{\rm pc}$. Taking this into account we get

$$\left(\frac{\delta\Omega}{\Omega}\right)_{\rm NIC} \simeq 0.09\, P f_\rho\, T_6^{-2} \left(\frac{B_0}{10^{12}\,{\rm G}}\right)^{-1} \tag{33}$$

$$\left(\frac{\delta\Omega}{\Omega}\right)^{\rm c}_{\rm NIC} \simeq 0.027\, P^{1/4} f_\rho^{1/2}\, T_6^{-1} \left(\frac{B_0}{10^{12}\,{\rm G}}\right)^{-1/2} \tag{34}$$

$$\left(\frac{\delta\Omega}{\Omega}\right)_{\rm CR} \simeq 0.023 \left(\frac{P}{0.3\,{\rm s}}\right)^{19/12} f_\rho^{1/2} \left(\frac{B_0}{10^{12}\,{\rm G}}\right)^{-5/6} \tag{35}$$

$$\left(\frac{\delta\Omega}{\Omega}\right)_{\rm RIC} \simeq 0.034\, P^{1/2} f_\rho^2\, T_6^{-4/3} \left(\frac{B_0}{1.2\times10^{13}\,{\rm G}}\right)^{-14/3}. \tag{36}$$

The temperature of the polar cap T due to the heating by return particles is of the order of 10^6 K. If the NS temperature is higher than this value, formula (33) should be applied; in the opposite case, formula (34) should be used. The temperature of the NS surface depends on the NS cooling model, and for a rather young pulsar it should be higher than 10^6 K. Thus, formula (33) is applicable for young, hot pulsars, where it gives for $\delta\Omega/\Omega \lesssim 0.01$. Hence, in the model with free particle escape, the ratio $\delta\Omega/\Omega$ is of the order of a few per cent for the majority of pulsars.

We see that $1-\beta$ is of the order of a few per cent for most pulsars in the model with free particle escape and for young pulsars in the model with no particle escape. We restrict ourselves to considering only pulsars where $1-\beta$ is small. Then the last term in pulsar equation (38) is small in comparison with other terms and can be neglected. In the rest of the paper we assume

$$\Omega_{\rm F} \equiv \Omega\,. \tag{37}$$

This assumption simplifies the pulsar equation (20), which now has the form

$$(x^2-1)(\partial_{xx}\psi + \partial_{zz}\psi) + \frac{x^2+1}{x}\partial_x\psi - SS' = 0\,, \tag{38}$$

where $S' \equiv {\rm d}S/{\rm d}\psi$. Non-linearity in this equation is now present only in the term with the poloidal current function S.

2.3 Poloidal current *S*

In contrast to $\Omega_{\rm F}$, being set by kinetic processes in the polar cap, S depends on the global structure of the magnetosphere. Both inside and outside the LC the pulsar equation (38) is a regular non-linear PDE of elliptic type. At the LC this equation under assumption (37) has the form

$$\partial_x\psi = \frac{1}{2}SS'\,. \tag{39}$$

If the function S is known, condition (39) can be considered as a Neumann-type boundary condition at the LC. If boundary conditions are set both inside and outside the LC, the equation should have an unique solution in both regions. Generally speaking, for an arbitrary function S the solutions of the pulsar equation inside and outside the LC will not match:

$$\lim_{x\to1^-}\psi \neq \lim_{x\to1^+}\psi\,. \tag{40}$$

Therefore a smooth[3] solution is possible only for a specific function S and the problem of finding a solution of the pulsar equations becomes an eigenvalue problem for the function S.

The position of the LC is not known a priori. For values of $\Omega_{\rm F}$ different from Ω it has a rather complicated form and, even if $\Omega_{\rm F}(\Psi)$ as a function of Ψ is given by a model of the polar cap cascade, the position of the LC as a function of x and z has to be found self-consistently together with the solution of the pulsar equation. However, as was stressed above, for most pulsars the deviation of the LC from a cylinder with radius c/Ω is of the order of a few per cent or less. Hence, a solution of equation (38) should give a very good approximation to the real magnetosphere of an aligned rotator.

The other open question regarding the poloidal current term in the pulsar equation is the topology of the magnetosphere. In works of the Lebedev Physical Institute group (see e.g. Beskin, Gurevich & Istomin 1993; Beskin & Malyshkin 1998), a geometry with an X null point has been assumed (hereafter X-configuration, see Fig. 13a). In that case the pulsar equation should be solved in three different domains, separated by the current sheets. The positions of the point A (and A') is a free parameter of such a model. In setting the positions of these points and the point x_0, one fixes the boundaries and gets a well posed, although complicated, problem. Such topology of the aligned rotator magnetosphere was criticized by Lyubarskii (1990), because the only source of the magnetic field in the magnetosphere is the pulsar itself, and in this case it is not clear what would be the source of the magnetic field in the outer domain. The most frequently considered topology of the aligned rotator magnetosphere implies a Y-like null point (hereafter a Y-configuration, see Fig. 1). In this case the only available free parameter in the model is the position of the null point x_0. By fixing the position of this point we fix the whole geometry of the magnetosphere. Thus we have an elliptic equation with boundary conditions set at all boundaries of the closed

[3] If the solution is continuous, its smoothness follows from equation (39), because SS' is the same at both sides of the LC.

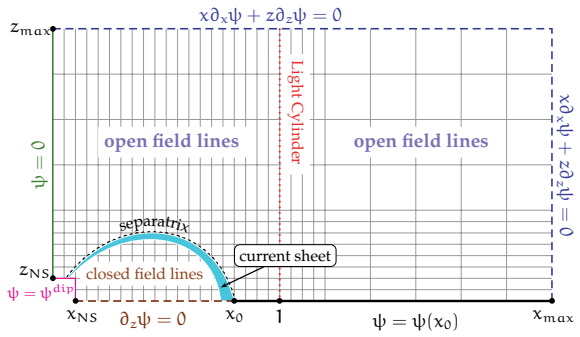

Figure 2. Calculation domain and imposed boundary conditions. See text for explanation.

domains with known positions of the boundaries. We wish to emphasize here that the choice of the topology of the magnetosphere is an additional assumption in the frame of the stationary problem. In the following we investigate in detail the force-free magnetosphere of an aligned rotator assuming topology with a Y-like neutral point.

3 NUMERICAL MODEL

We solve equation (38) in a rectangular domain, see Fig. 2. The boundary conditions are as follows. On the rotation axis (z-axis)

$$\psi(0, z) = 0, \qquad z_{NS} < z \leqslant z_{max}\,. \tag{41}$$

At the equatorial plane, in the closed field line zone

$$\partial_z\psi(x, 0) = 0, \qquad x_{NS} < x < x_0\,, \tag{42}$$

following from the symmetry of the system. In the open field line domain

$$\psi(x, 0) = \psi(x_0, 0), \qquad x_0 < x \leqslant x_{max}\,, \tag{43}$$

i.e. the separatrix lies in the equatorial plane. Close to the NS the magnetic field is assumed to be dipolar, so for $x = x_{NS}$, $0 \leqslant z_{NS}$ and $0 \leqslant x \leqslant x_{NS}$, $z = z_{NS}$

$$\psi(x, z) = \psi^{dip}(x, z) \equiv \frac{x^2}{(x^2 + z^2)^{3/2}}\,. \tag{44}$$

Magnetic surfaces should become radial at large distances from the NS, see Ingraham (1973). On the other hand, in the calculations of Contopoulos et al. (1999), where the pulsar equation was solved in the unbounded domain, with boundary conditions at infinity implying the finiteness of the total magnetic flux, the magnetic surfaces became nearly radial already at several sizes of the LC. Rather different outer boundary conditions, with a finite magnetic flux inside the LC at infinity, have been used by Sulkanen & Lovelace (1990). However, the time-dependent simulations of Komissarov (2006), Spitkovsky (2005) and McKinney (2006) provide strong evidence for the correctness of the outer boundary conditions when magnetic surfaces at large distances from the NS are radial. Thus, at the outer boundaries of the calculation domain for $0 < x \leqslant x_{max}$, $z = z_{max}$ and $x = x_{max}$, $0 < z \leqslant z_{max}$

$$x\,\partial_x\psi + z\,\partial_z\psi = 0. \tag{45}$$

At the LC two conditions should be satisfied: (i) the solution should be continuous,

$$\psi(x \to 1^-, z) = \psi(x \to 1^+, z)\,, \tag{46}$$

and (ii) the condition (39). These conditions together provide a smooth transition through the LC. Following Goodwin et al. (2004) we expand the function ψ at the LC in the Taylor series over x, imposing the continuity condition (46). By substituting the resulting expansion into the pulsar equation (38) and retaining the terms up to the second order we get the following approximation to the pulsar equation at the LC:

$$4\partial_{xx}\psi(1, z) + 2\partial_{zz}\psi(1, z) = \partial_x[SS'(1, z)]\,. \tag{47}$$

This equation is nothing more than a reformulation of the smoothness conditions (46) and (39), valid for the first- and second-order terms in the Taylor series expansion of ψ. As the numerical scheme we have used is of the second order, this approximation, as well as its discretization, has the same accuracy as the discretized equation in the rest of the numerical domain. In the course of the relaxation procedure we are trying to satisfy the conditions (46) and (39), i.e. we solve equation (47) at the LC instead of the original equation (38), which is singular there. Equation (39) is used for the determination of the poloidal current term $SS'(\psi)$ along the open field lines.

In the closed field lines zone, $\psi > \psi_{last} \equiv \psi(x_0, 0)$, there is no poloidal current, so $SS' \equiv 0$. The return current needed to keep the system charge neutral flows along the separatrix. In the open field line domain for $x > x_0$, the presence of an infinite thin current sheet is already incorporated into the solution procedure by setting the boundary condition (43). However, when the separatrix goes above the equatorial plane we have to model the current sheet. We assume that the return current is flowing along the field lines corresponding to the magnetic surfaces $[\psi_{last}, \psi_{last} + d\psi]$. The total return current flowing in this region is calculated by integrating the term SS':

$$S_{return} = \sqrt{2\int_0^{\psi_{last}} SS'\,d\psi}\,. \tag{48}$$

We model the poloidal current density distribution over ψ in the current sheet $\psi_{last} \leqslant \psi \leqslant \psi_{last} + d\psi$ by an even-order polynomial function going to zero at the boundaries of the current sheet

$$S'(\psi) = A\left\{\left[\psi - \left(\psi_{last} + \frac{d\psi}{2}\right)\right]^{2k} - \left(\frac{d\psi}{2}\right)^{2k}\right\}, \tag{49}$$

where the constant A is determined from the requirement $\int_0^{\psi_{last}+d\psi} S(\psi)\,d\psi = 0$ and k is an integer constant. The pulsar equation is then solved in the whole domain including the current sheet. The current sheet cannot be considered as a force-free domain, but in doing so we correctly calculate the influence of the current sheet on to the global magnetospheric structure, even though the obtained values of the physical parameters *inside* the current sheet are fake.

We developed a multigrid numerical scheme for the solution of equations (38) and (47). These equations have been discretized using the five-point Gauss–Seidel rule. The coarsest numerical grid was constructed in such a way that the LC is at the cell boundaries. Each subgrid was obtained by halving the previous grid. Cell sizes in the region $x < 1$, $z < 1$ are smaller in order to accurately calculate the current along the separatrix. We use the Full Approximation Scheme with V-type cycles (see Trottenberg et al. 2001). The Gauss–Seidel scheme was used as both a smoother and a solver at the coarsest level. At each iteration step, both in the solver and the smoother, the new value of the poloidal current term $SS'(1, z)$ was calculated from the relation (39) at each point of the LC. Then a piece-polynomial interpolation of SS' in the interval $(0, \psi_{last})$ was constructed and the return

Table 1. Properties of obtained solution with $x_0 = 0.7$ and x_0 approaching the LC for different values of numerical parameters.

Numerical parameters				Results	
$d\psi$	$2k$	$(x_{\max}, z_{\max})$	(x_{NS}, z_{NS})	$\psi_{\rm last}$	W
$x_0 = 0.7$					
0.03	2	(8, 7)	(0.0667, 0.056)	1.717	1.864
0.03	4	(8, 7)	(0.0667, 0.056)	1.712	1.853
0.015	2	(8, 7)	(0.0667, 0.056)	1.697	1.821
0.03	2	(8, 7)	(0.0333, 0.028)	1.720	1.870
0.03	2	(16, 14)	(0.0667, 0.056)	1.717	1.864
$x_0 = 0.99$					
0.08	2	(16, 14)	(0.06, 0.06)	1.255	0.977
$x_0 = 0.99231$					
0.04	2	(5, 5)	(0.0462, 0.0525)	1.230	0.939

current distribution was calculated according to the formulae (48) and (49). Then for each point (x, z) in the calculation domain the current term was calculated as $SS'(x, z) = SS'[\psi(x, z)]$, and the new iteration was started. Thus we solved the pulsar equation in the whole domain while avoiding a very time-consuming matching of the solutions inside and outside the LC, as was done by Contopoulos et al. (1999), Contopoulos (2005) and Gruzinov (2005), though in Contopoulos (2005) this matching procedure has been accelerated. As a starting configuration, a dipolar magnetic field everywhere was used. We did not encounter any problems with the convergence of the scheme for any value of x_0, but for x_0 very close to 1 the convergence rate becomes essentially slower. The typical number of points we used along each direction in the calculations was 3000–6000.

We performed calculations for different values of numerical parameters in order to proof the independence of the results on the domain sizes $(x_{\max}, z_{\max})$, the 'NS size' $(x_{\rm NS}, z_{\rm NS})$, the width of the current sheet $d\psi$ and the form of the current distribution (parameter k), as well as on the iteration procedure stopping criteria and the number of points in both directions. Changes in convergence criteria and the decrease of the cell size from those used in most of our calculations did not produce relative changes in solutions greater that 10^{-4}. In Table 1 values of $\psi_{\rm last}$ and the energy losses of an aligned rotator W (see next section), obtained in computations with different values of listed numerical parameters, are shown for $x_0 = 0.7$ and x_0 approaching the LC. One can see that, with an accuracy of the order of a few per cent, obtained solutions are independent of particular values of the numerical parameters. Solutions with other x_0 values show similar behaviour.

4 RESULTS OF CALCULATIONS

Our choice of the boundary conditions at the NS, equation (44), corresponds to the case when the dipole magnetic moment of the star $\boldsymbol{\mu}$ is parallel to the angular velocity vector $\boldsymbol{\Omega}$, $\boldsymbol{\mu}||\boldsymbol{\Omega}$. In this case the GJ charge density in the polar cap of the pulsar is negative and electrons flow away from the polar cap. The poloidal current S in the open field line zone is negative (see the definition of the poloidal current in equation 8). In the case of an anti-aligned rotator, i.e. $\boldsymbol{\mu}$ is antiparallel to $\boldsymbol{\Omega}$, all signs of the physical quantities related to the charge and current should be reversed.

Calculations have been performed for the following values of x_0: 0.15, 0.2, 0.3, 0.4, 0.5, 0.6, 0.7, 0.8, 0.9, 0.95, 0.99 and 0.992. A unique solution has been found for each of the above x_0 values.

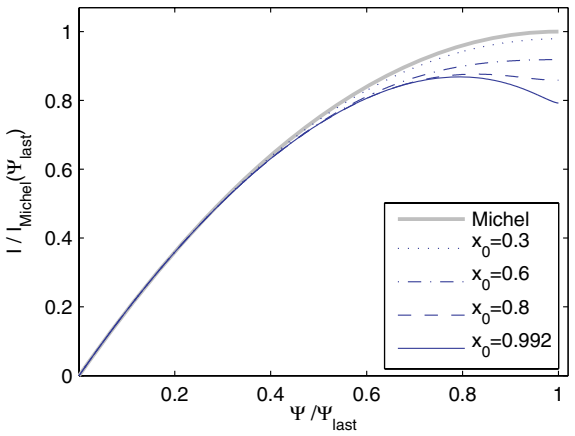

Figure 3. The poloidal current distribution in the open field line zone normalized to the poloidal current from the corresponding Michel solution. Inside the current sheet, for $\psi_{\rm last} \leqslant \psi \leqslant \psi_{\rm last} + d\psi$ (not shown here), the poloidal current decreases to 0.

Let us consider in detail the physical properties of the obtained solutions.

4.1 Poloidal current

The poloidal current density S, calculated from the formula (48), does not deviate by more than ∼20 per cent from the values given by Michel's solution (Michel 1973b)

$$S = -\psi \left(2 - \frac{\psi}{\psi_{\rm last}}\right), \tag{50}$$

see Fig. 3. The smaller x_0, the smaller this deviation. The structure of the magnetosphere depends strongly on the poloidal current distribution. In solutions with $x_0 \gtrsim 0.6$ there is a domain in the open filed line zone, where *volume* return current flows. However, only a small part of the return current flows there; the main part flows inside the current sheet. The size of this domain gets smaller with decreasing x_0, and for $x_0 \lesssim 0.6$ the return current flows only along the separatrix, see Fig. 4. Qualitatively this property of the solution could be explained as follows. At the LC the condition (39) is satisfied, so if $\partial_x\psi$ changes sign the same occurs with the current term SS', and the poloidal current density changes sign. Magnetic field lines close to the null point are bent towards the equatorial plane, but at large distances they become radial. Therefore, for x_0 close to 1$\partial_x\psi\ (1, z) < 0$ for some field lines and volume return current must flow along them. When x_0 decreases, more and more magnetic field lines at the LC will be bent away from the equatorial plane until there will be no lines bent towards the equator. If field lines at the LC bend from the the equatorial plane $\partial_x\psi\ (1, z) > 0$ and there is no volume return current along such field lines.

A convenient representation of the current density in the closed field line zone could be given by the current density distribution in the polar cap $j_{\rm pc}$. In our notations the current density in the polar cap of pulsar normalized to the GJ current density $j_{\rm GJ} \equiv \rho_{\rm GJ}c$ is given by (see Appendix A, equation A6)

$$j_{\rm pc} = |j_{\rm GJ}|\ \frac{1}{2}S' \left[\left(\frac{\theta}{\theta_{\rm pc}}\right)^2 \psi_{\rm last}\right], \tag{51}$$

where $\theta/\theta_{\rm pc}$ is the colatitude normalized to the colatitude of the polar cap boundary $\theta_{\rm pc}$; it is connected to the function ψ through

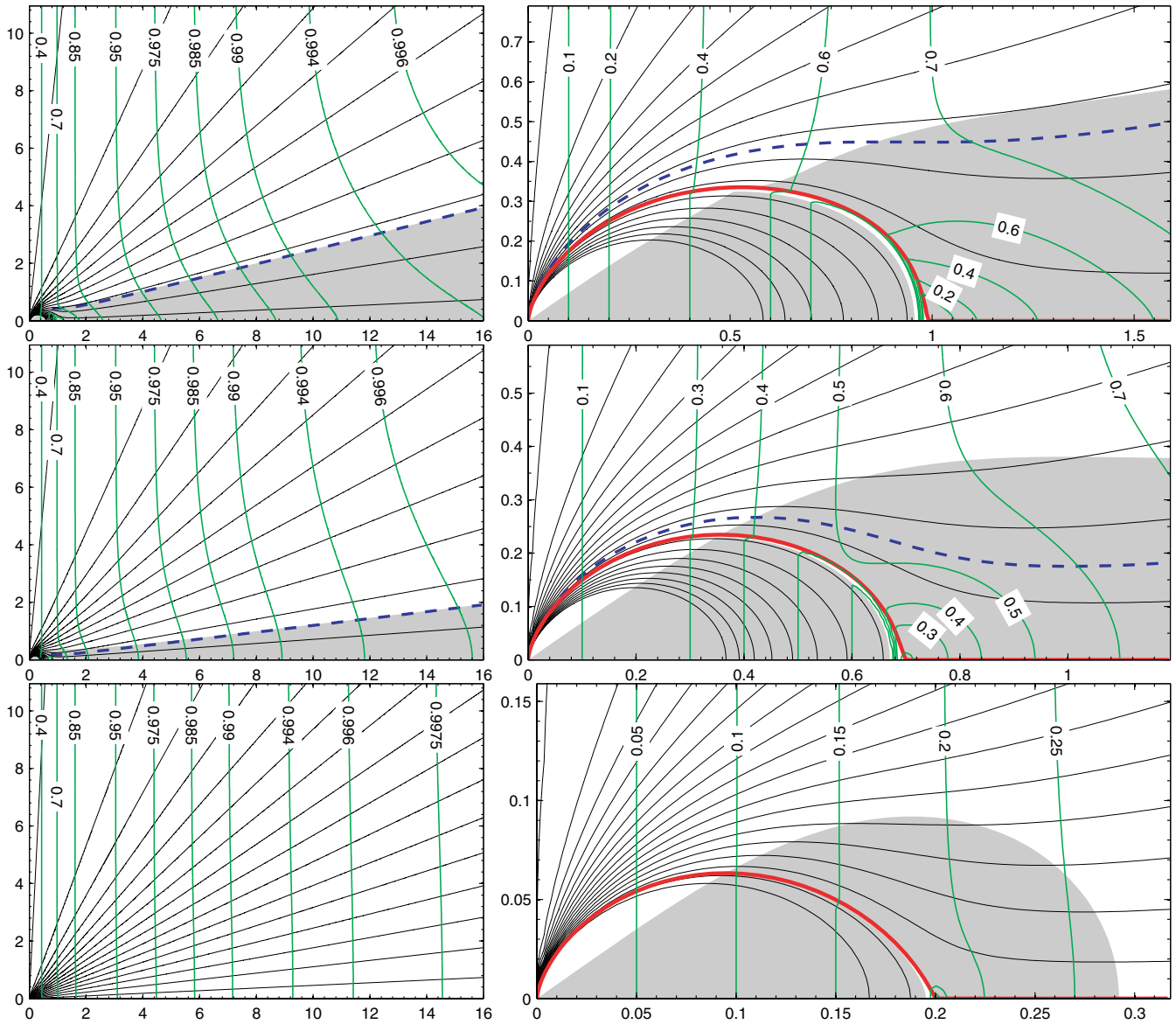

Figure 4. Global structure of the magnetosphere for $x_0 = 0.992$ – top panels, $x_0 = 0.7$ – middle panels, $x_0 = 0.2$ – bottom panels. The magnetic flux surfaces are shown by thin solid lines, the labelled vertical lines are contours of the drift velocity and the grey area is the domain where the GJ charge density is positive. The dashed line separates regions with direct (above the line) and return (below the line) volume currents. The separatrix is shown by the thick solid line. Almost the whole calculation domain is shown in the left-hand panels, and the central part of the calculation domain is shown in the right-hand panels. Distances along x-axis (horizontal) and z-axis (vertical) are measured in units of LC radius $R_{\rm LC}$.

the relation $\theta/\theta_{\rm pc} = \sqrt{\psi/\psi_{\rm last}}$. In Fig. 5 $j_{\rm pc}$ is shown for several solutions with different x_0 values. The current density never exceeds the corresponding GJ current density and goes to zero at the polar cap boundary. The latter property is the consequence of the assumed topology of the magnetosphere. Indeed, from the condition at the LC, equation (39), the current density along a given magnetic surface is proportional to the partial derivative $\partial_x\psi$ at the LC, but in configurations with the Y null point $\partial_x\psi = 0$ for $\psi = \psi_{\rm last}$. The deviation of the current density $j_{\rm pc}$ from the GJ current density increases close to the polar cap boundaries with increasing x_0. For solutions with $x_0 \gtrsim 0.6$ the current density $j_{\rm pc}$ changes sign at some point near the boundary. On the other hand, $j_{\rm pc}$ never exceeds the corresponding Michel current density and approaches $j_{\rm Michel}$ when x_0 decreases.

4.2 Drift velocity and force-free approximation

The drift velocity in our notations is given by

$$u_{\rm D} \equiv \frac{|\boldsymbol{U}_{\rm D}|}{c} = \frac{\Omega\varpi}{c}\frac{B_{\rm pol}}{B} = \frac{x}{\sqrt{1+\frac{S^2}{(\partial_x\psi)^2+(\partial_z\psi)^2}}}, \qquad (52)$$

$B_{\rm pol}$ is the poloidal component of the magnetic field. The light surface, i.e. the surface where the force-free approximation breaks down, coincides with the surface, where $u_{\rm D} = 1$. We verified the applicability of the force-free approximations in each case. For most of the cases the calculations have been performed in the domain with $x_{\rm max} = 8$, $z_{\rm max} = 7$, but for $x_0 = 0.2, 0.7, 0.992$ we also performed calculations with $x_{\rm max} = 16$, $z_{\rm max} = 14$. In all cases the light surface

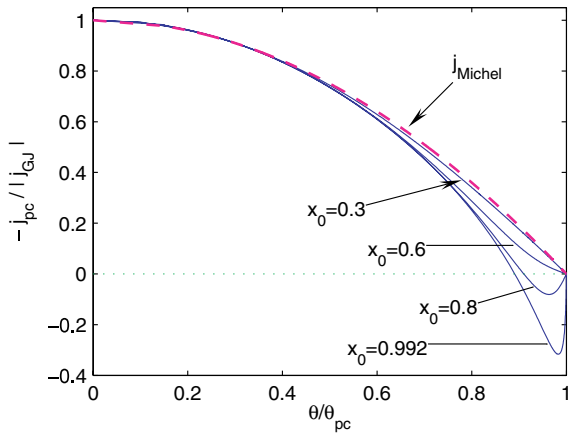

Figure 5. Current density distribution in the polar cap of pulsar $j_{\rm pc}$ as a function of the colatitude. $j_{\rm pc}$ is normalized to the GJ current density $|j_{\rm GJ}|$ and the colatitude is measured in units of the polar cap boundary colatitude $\theta_{\rm pc}$.

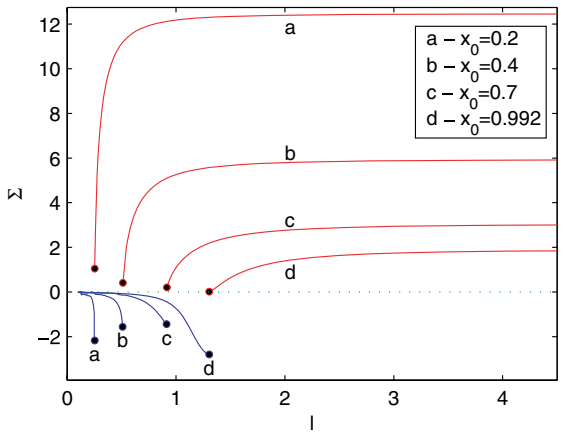

Figure 6. Σ – linear charge density of the current sheet (see text) as a function of the distance l *along* the current sheet. Σ is normalized to $0.5\,\mu/R_{\rm LC}^2$. l is measured in units of $R_{\rm LC}$. The points marks the position of the corresponding null point. Note the jump in the charge density at these points. The dotted line corresponds to $\Sigma = 0$.

is located somewhere outside of these domains (see Fig. 4). The drift velocity distribution for the solutions with x_0 close to 1, even at large distances from the null point, differs significantly from that in the corresponding Michel solution (the solution with the same $\psi_{\rm last}$), where the drift velocity is the function of only the x-coordinate. On the other hand, when x_0 decreases, $u_{\rm D}$ approaches the values from the corresponding Michel solution.

4.3 Charge distribution in the magnetosphere

The GJ charge density in the magnetosphere in our notation is given by

$$\rho_{\rm GJ} = \rho_0\,\frac{SS' - \frac{2}{x}\,\partial_x\psi}{1-x^2}\,, \qquad \rho_0 \equiv \frac{\mu}{4\pi R_{\rm LC}^4}\,. \tag{53}$$

Close to the rotation axis the GJ charge density is negative and with increasing of the colatitude it becomes positive. While for the solutions with $x_0 \gtrsim 0.6$ the domain of positively charged plasma extends to infinity, for the solutions with smaller x_0 values it becomes finite (cf. plots for $x_0 = 0.2$ with other plots in Fig. 4). The reason for this is as follows. At large distances from the LC the magnetic field lines becomes radial, so $\partial_x\psi$ is always greater than 0. Hence, there only the term SS' is responsible for changing of the charge density sign. However, SS' for $x_0 \lesssim 0.6$ never changes sign (see left-hand plots in Fig. 4). For the same reason the volume return current always flows trough the positively charged domain. Close to the NS it passes trough the layer where charge density changes sign (see right-hand plots in Fig. 4). At this layer the so-called outer-gap cascade should develop (see e.g. Cheng, Ruderman & Sutherland 1976; Takata, Shibata & Hirotani 2004).

The force-free solution fixes not only the volume charge density, but also the charge density of the current sheet. As the electric field at opposite sides of the current sheet is different, the current sheet must have non-zero surface charge density. In Fig. 6 we plot the linear charge density Σ of the current sheet as a function of distance l along the separatrix

$$\Sigma \equiv 2\pi\varpi\,\sigma\,, \tag{54}$$

where σ is the charge density of the current sheet. Σ represents the total charge of a volume that is co-moving with particles flowing along the separatrix with constant speed, emitted at the same time (either at the NS or at 'infinity'). $\Sigma \equiv$ constant would imply a constant velocity flow of particles of *one* sign. However, for each solution Σ is a non-monotonic function with discontinuity in the null point. Such a complicated dependence of Σ on l implies some non-trivial physics connected with particle creation in the current sheet, which is discussed in the next section.

This complicated dependence of the current sheet charge density is easy to understand if one consider the so-called 'matching condition' at the separatrix. As was shown by Lyubarskii (1990),[4] at the current sheet the following condition for the electric and magnetic field in closed (c) and open (o) field line domains should be satisfied

$$E_{\rm c}^2 - B_{\rm c}^2 = E_{\rm o}^2 - B_{\rm o}^2\,. \tag{55}$$

This follows from the integration of equation (6) across the current sheet. In the closed field line zone there is no toroidal magnetic field. It follows from equations (14) and (8) that the electric field

$$E = x B_{\rm pol}\,. \tag{56}$$

Substituting this equation into equation (55), we get

$$B_{\rm pol,\,c}^2 - B_{\rm pol,\,o}^2 = \frac{B_{\phi,{\rm o}}^2}{1-x^2}\,. \tag{57}$$

From this and equation (56) it follows that $E_{\rm c} > E_{\rm o}$ and that the charge density in the current sheet between the closed and open field line domains,

$$\sigma = \frac{1}{4\pi}(E_{\rm o} - E_{\rm c})\,, \tag{58}$$

is always *negative*. On the other hand, from the symmetry of the system – the electric field in regions [2] and [2′] in Fig. 1 has different directions – the charge density of the current sheet in the open field line zone

$$\sigma = \frac{1}{2\pi}E_{\rm o} \tag{59}$$

is always *positive*.

The total charge of the system, i.e. the charge of the NS, the magnetosphere and the current sheet together, must be zero. The boundary condition (45) implies that the total flux of electric field

[4] See also Okamoto (1974), equation (69).

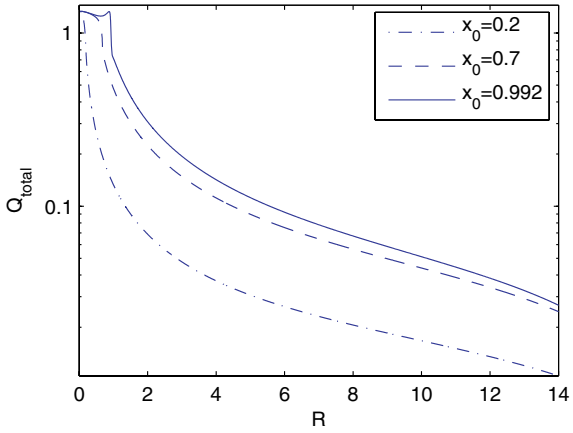

Figure 7. The total charge inside the sphere of the radius R centred at the NS: charge of the NS + charge in the magnetosphere obtained by direct integration of $\rho_{\rm GJ}$. $Q_{\rm total}$ is normalized to $0.5\,\mu/R_{\rm LC}$. R is measured in units of $R_{\rm LC}$.

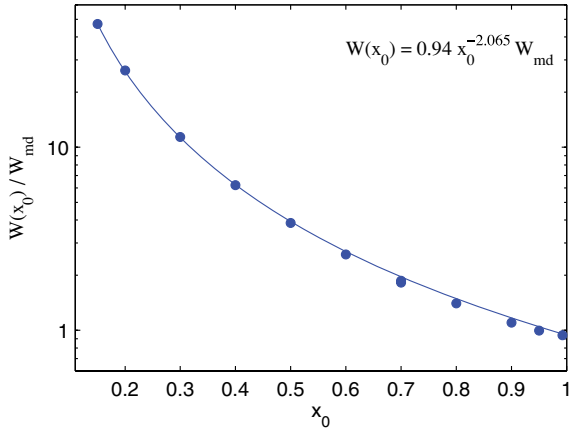

Figure 8. Energy losses of the aligned rotator as a function of x_0 in units of the corresponding magnetodipolar energy losses $|W_{\rm md}|$.

through the sphere of a large radius is zero, hence the total charge of the system must be zero. In Fig. 7 the total charge inside the sphere centred at the coordinate origin is plotted as a function of its radius. The total charge of the system goes rapidly to zero at large distances from the NS. This plot could be also considered as an additional test of the numerical procedure, as the conservation of the total charge is not incorporated into the numerical scheme.

4.4 Energy losses

Energy losses of the aligned rotator in our notations are given by the formula

$$W = |W_{\rm md}| \int_0^{\psi_{\rm last}} S\,{\rm d}\psi\,, \tag{60}$$

where $|W_{\rm md}|$ is the absolute value of magnetodipolar energy losses, here defined as

$$|W_{\rm md}| = \frac{B_0^2 R_{\rm NS}^6 \Omega^4}{4c^3}\,; \tag{61}$$

see Appendix B, equations (B7) and (B5). In the obtained set of solutions, W is a function of x_0. As x_0 decreases, the amount of open magnetic field lines increases and, as the poloidal current dependence on ψ does not change substantially, the energy losses of an aligned rotator increase with decreasing x_0, see Fig. 8. The obtained dependence of energy losses W on the position of the null point x_0 could be surprisingly well fitted by a single power law:

$$W(x_0) \approx -0.94\,x_0^{-2.065}\,|W_{\rm md}|\,. \tag{62}$$

This formula is similar to the one obtained from analytical estimations using the Michel current distribution (see Appendix B, equation B9)

$$W(x_0) \approx -\frac{2}{3}x_0^{-2}\,|W_{\rm md}|\,. \tag{63}$$

The angular distribution of the energy flux (see Appendix B, equation B4) is

$$\frac{{\rm d}W}{{\rm d}\omega} = \frac{|W_{\rm md}|}{4\pi}\,S\frac{\sqrt{x^2+z^2}}{x}\,(z\,\partial_x\psi - x\,\partial_z\psi)\,. \tag{64}$$

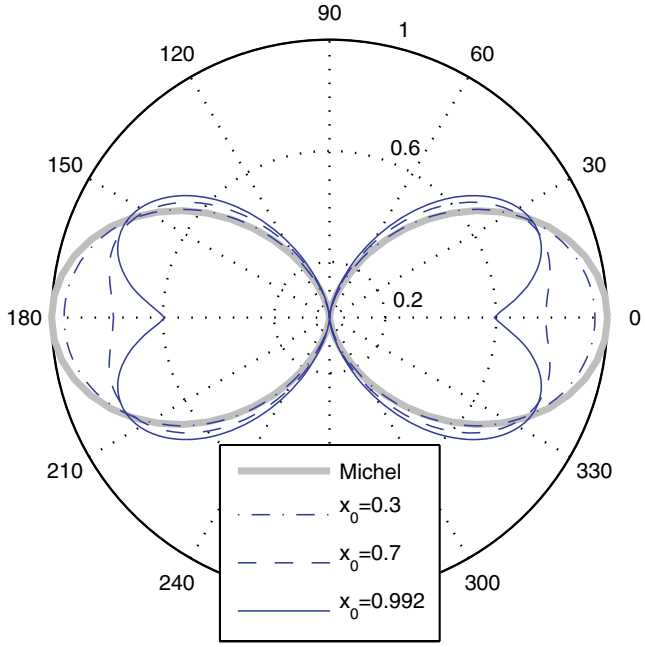

Figure 9. Angular distribution of the energy flux ${\rm d}W/{\rm d}\omega$ normalized to $-\psi_{\rm last}^2\,|W_{\rm md}|/(4\pi)$, see equations (64) and (65). The distributions shown here are taken at $R = 4R_{\rm LC}$ and correspond to their asymptotic forms (see the text).

In Fig. 9 this distribution is shown for several solutions with different x_0. The Poynting flux distribution quickly reaches its asymptotic form at distances from the null point of the order of 1–2 $R_{\rm LC}$. For example, in the case of $x_0 = 0.99$ distributions taken at $R = 4$ and $R = 14$ differ by no more than ∼3 per cent. For configurations with smaller x_0 values this deviation is even less. The smaller the value of x_0, the closer the angular energy flux distribution to the angular distribution in Michel's solution:

$$\frac{{\rm d}W}{{\rm d}\omega} = -\frac{|W_{\rm md}|}{4\pi}\,\psi_{\rm last}^2\sin^2\theta\,, \tag{65}$$

because for small x_0 the solution at large distances is very close to the Michel solution. In spite of recent works on modelling of jet-torus structure seen in Crab and other plerions (see Komissarov

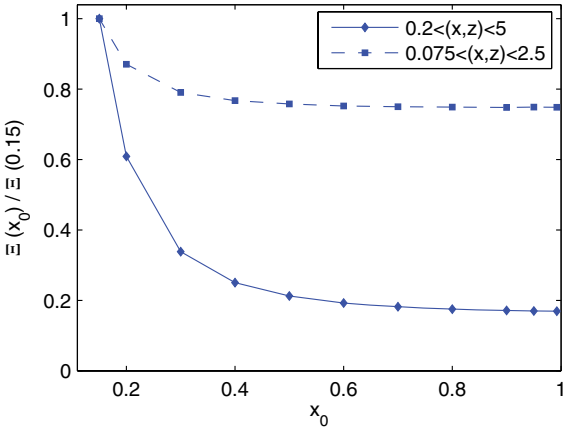

Figure 10. Total energy of electromagnetic field in two different volumes of fixed sizes as a function of x_0. Ξ is normalized to the corresponding value of $\Xi(x_0 = 0.15)$.

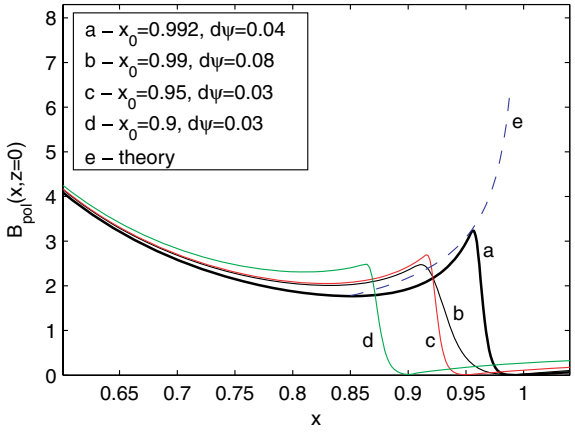

Figure 11. Poloidal magnetic field strength in the equatorial plane as the function of x. $B_{\rm pol}$ is normalized to $\mu/R_{\rm LC}^3$. By the dashed line the theoretical prediction for $B_{\rm pol}(x, 0)$ is shown for the solution with $x_0 = 0.992$, equation (66).

& Lyubarsky 2003; Bogovalov et al. 2005), we note that magnetosphere configurations with larger x_0 would support more strongly the development of instabilities due to more asymmetric energy deployment into the plerion, providing a more pronounced disc structure.

4.5 Total energy of the magnetosphere

The total energy of electric and magnetic fields in the magnetosphere $\Xi \equiv \int (B^2 + E^2)/(8\pi)\,{\rm d}V$ would give information on which configuration the system tries to achieve; the configuration with the minimal possible energy. Obviously for the obtained solutions we could calculate the energy only in a finite domain. Another problem is the very rapid increase of the magnetic field in the central parts, as r^{-3}. As the magnetic field close to the NS is dipolar for each configuration, we calculate the total energy in a domain excluding the central parts. In order to verify the independence of the result on domain sizes we calculate the total energy in the magnetosphere in two different domains for each solution. These domains are defined as $0.2 \leqslant x \leqslant 5$, $0.2 \leqslant z \leqslant 5$ and $0.075 \leqslant x \leqslant 2.5$, $0.075 \leqslant z \leqslant 2.5$ The results are plotted as a function of x_0 in Fig. 10. The total energy of the magnetosphere increases with decreasing x_0, so the magnetosphere will try to achieve the configuration with the maximum possible x_0.

4.6 Solution with $x_0 \to 1$

The special case of $x_0 \to 1$ has been considered by several authors, because it was believed to be the real configuration of a pulsar magnetosphere (Lyubarskii 1990; Contopoulos et al. 1999; Uzdensky 2003; Gruzinov 2005; Komissarov 2006). This case is peculiar in the sense, that magnetic field in the closed filed line zone diverges in the Y null point. Indeed, from equation (57) it follows that near the null point, when $x_0 \to 1$

$$B_{\rm pol} \approx \frac{\mu}{R_{\rm LC}^3} \frac{|S|}{\sqrt{2(1-x)}}. \qquad (66)$$

While the presence of the singularity was noted by Lyubarskii (1990) and Uzdensky (2003), Gruzinov (2005) firstly realized that such singularity is admitted, as it does not lead to the infinite energy of magnetic field in the region surrounding the null point. In Fig. 11 the strength of the poloidal magnetic field along the x-axis is plotted for different solutions. By the dashed line the relation (66) is shown. We see that when x_0 approaches the LC the magnetic field inside the closed zone begins to grow close to the null point. This increase is more pronounced when the thickness of the current sheet decreases. Agreement between the curve for $x_0 = 0.992$, $d\psi = 0.4$ and the dashed line is quite good.

Gruzinov (2005) solved an equation for the separatrix in the vicinity of the null point $x_0 = 1$ and have found that the angle at which separatrix intersects the equatorial plane should be 77.3°. In our calculations we found this angle to be ≈78° for $x_0 = 0.992$, $d\psi = 0.04$ and ≈70° for $x_0 = 0.99$, $d\psi = 0.08$. So, our numerical solution shows good agreement with the analytical one. Energy losses found by Gruzinov (2005) are 1.0 ± 0.1, what quite good agrees with values for W from Table 1. Value of $\psi_{\rm last} = 1.23$ calculated by Contopoulos (2005) coincide with ones from Table 1 and is close to $\psi_{\rm last} = 1.27$ obtained by Gruzinov (2005), although both of these results have been obtained with codes having worse numerical resolution than the code used in this work.

5 DISCUSSION

It seems natural to assume that force-free configurations are energetically preferably in comparison with configurations where there are geometrically large volumes with parallel electric field.[5] Accepting this, we conclude that the magnetosphere of a pulsar should evolve through a set of force-free configurations. It does not necessarily mean that for a relatively short transition time the system could not be essentially non-force-free, but rather that for most of the time the magnetosphere of an active pulsar is force-free.

5.1 Polar cap cascades and force-free magnetosphere

In a force-free configuration the current density distribution is not a free parameter; it is set by the structure of the magnetosphere, for example, by the value of x_0 in the case of Y-configuration. However, the current in the magnetosphere of the pulsar is supported by electron–positron cascades in the polar cap, i.e. most of the current carriers are produced in the magnetosphere and are not supplied

[5] However, see e.g. Smith et al. (2001) or Pétri et al. (2002).

from external sources. Independently of neutron star crust properties, i.e. whether or not charged particles could be extracted from the surface, in the polar cap of young pulsars electron–positron cascades are developed, filling the magnetosphere of the star with particles (Ruderman & Sutherland 1975; Scharlemann et al. 1978; Muslimov & Tsygan 1992). Also, these particles are necessary in order to support the MHD-like structure of the magnetosphere. The current in the magnetosphere flows trough this cascade region, hence the cascade, the properties of which depend on the local magnetic field structure, has to adjust to the global properties of the magnetosphere too, namely to the current density flowing through it. We focus here on the case of stationary cascades. The hypothesis about the stationarity of the polar cap cascades, that the temporal variation of the accelerating electric field over the whole polar cap is much less than the accelerating field itself, is widely adopted (e.g. Daugherty & Harding 1982; Ruderman & Sutherland 1975). We briefly also address the case of essentially non-stationary cascades (Levinson et al. 2005).

As was shown by Lyubarskij (1992), for current adjustment in the stationary cascades a particle inflow from the magnetosphere into the cascade region is required. The typical current density, self-consistently supported by stationary polar cap cascades, is close to $j_{\rm GJ}$. For current densities, both larger or smaller than the GJ one, a particle inflow is necessary. The source of inflowing particles needed for current adjustment could be outer gap cascades, operating at the surface where the GJ charge density changes sign (Cheng et al. 1976). On the other hand, inflowing particles could be provided by the pulsar wind, where some outflowing particles could be reversed back to the NS due to momentum redistribution or due to a small residual electric field arising as the magnetosphere tries to support a force-free configuration. However, the zone where particles could flow *toward* the NS is limited by the LC (see Appendix C). Thus the source of inflowing particles must be inside the LC.

For Ruderman & Sutherland (1975) cascades, when particles can not be extracted from the NS surface and are produced in the discharge zone, the adjustment mechanism works as follows. An inflow of positrons increases the current density, and an inflow of electrons decreases it. In the first case the inflowing positrons decrease the charge density in the PFF and more electrons are necessary to adjust the charge density to the GJ value. These additional electrons, together with inflowing positrons, increase the current density. When there is an inflow of electrons, fewer primary electrons are necessary in order to support the GJ charge density at the PFF. Inflowing electrons are turned back at the PFF, and compensate the inflowing electric current. The outflowing current is only due to the primary electrons from the discharge zone, so the current density is less than $j_{\rm GJ}$.

If particles could almost freely escape from the NS crust, the pulsar must operate in the so-called space charge limited flow (SCLF) regime and the current density cannot be essentially less then $j_{\rm GJ}$. Indeed, the charge density in the discharge region, below the PFF, is close to $\rho_{\rm GJ}$ and the accelerating electric field forces charges to flow out with relativistic velocities (Scharlemann et al. 1978; Muslimov & Tsygan 1992). For cascades operating in the SCLF regime the mechanism of current adjustment works similarly for inflowing positrons. The particle inflow could *increase* the current density, but not decrease it. Only when the accelerating electric field is almost completely screened could the current density be significantly less than $j_{\rm GJ}$. However, in order to screen this accelerating field, charged particles flowing in from the magnetosphere must penetrate practically up to the NS surface, i.e. they must have Lorentz factors comparable to the Lorentz factors of particles accelerated in the polar gap. In other words, somewhere in the magnetosphere inside the LC there should be zone(s) where particles are accelerated as effectively as they would be accelerated in the polar cap. Either the accelerating field there should be comparable to the one in the polar cap or the size of this zone would be essentially larger than some NSs radii. Both seem to be inappropriate.

In both of these cases, in order to support the volume *return* current which flows in the direction opposite to $j_{\rm GJ}$, the accelerating field in the polar cap discharge zone must be completely screened and the particles filling the magnetosphere along magnetic field lines with return volume current must be produced somewhere in the magnetosphere. The accelerating electric field in the polar cap zone, being proportional to the magnetic field strength, is much stronger than any possible accelerating electric field far from the NS. Hence, the presence of the return volume current in the force-free magnetosphere seems to be incompatible with the force-free configurations of the magnetosphere, because the acceleration of particles to the required Lorentz factors with a much weaker electric field requires large non-force-free domain(s) in the magnetosphere. The situation with non-stationary cascades is poorly investigated; currently there is only one work dedicated to detailed studies of significantly non-stationary cascades – Levinson et al. (2005). However, we see no way how it would be impossible to support both particle production in the polar cap cascade and an average current that has an opposite direction to the direction of the accelerating electric field; see also Arons (1979).

In our consideration we assumed that the GJ charge density in the polar cap does not deviate substantially from its canonical value (Goldreich & Julian 1969)

$$\rho_{\rm GJ} = -\frac{\Omega B_0}{2\pi c}\,. \tag{67}$$

This is the case when the boundary of the polar can be considered as equipotential, i.e. having very high conductivity. However, if its conductivity is very low and the surface charge density distribution at the separatrix in the polar cap is different from the one in the force-free solution, the GJ charge density can substantially deviate from values given by formula (67). In this case the characteristic current density flowing trough the cascade region would be different from the canonical value of $-(\Omega B_0)/(2\pi)$ and, in principal, it could approach the values required by the global magnetospheric structure, i.e. the problem of current adjustment could be solved by modifying $\rho_{\rm GJ}$ instead of adjusting the deviation of j from $j_{\rm GJ}$. Let us analyse this possibility. The largest part or the whole of the return current flows along the separatrix. It could be electrons returning from the region behind the light surface[6] or ions outflowing from the NS surface (see e.g. Spitkovsky & Arons 2004). If there are electrons in the current sheet close to the NS, then a substantial deviation of the electric field from the force-free value will give rise to electron–positron cascades that produce enough particles to make the separatrix near equipotential. Only ions, which emit photons capable to produce electron–positron pairs less effectively, could support an essentially non-equipotential polar cap boundary. However, as was mentioned before, each particularly force-free configuration fixes the surface charge density distribution along the current sheet everywhere where it is applicable. Independently of the detailed structure of the polar cap zone, the surface charge density along the separatrix between closed and open field lines is *negative*, i.e. there must be enough electrons there, or the magnetosphere would be not force-free (see

[6] The current sheet is not a force-free domain and considerations from Appendix C are not valid here.

Section 4.3 and Fig. 6). Although in the discharge zone above the polar cap the force-free approximation is not valid, and the arguments of Section 4.3 cannot be directly applied to the current sheet at the polar cap boundaries, electrons must be there for the following reason. The current sheet is a region where the force-free approximation is broken, at least in some places (for example in the null point, where the surface charge density is discontinuous). As the return current flows in the current sheet, the parallel electric field will be directed from the NS, accelerating electrons in the current sheet toward the NS surface. Hence there are also electrons in the current sheet at the polar cap boundary, and this boundary will be approximately equipotential. Consequently, the GJ charge density in the polar cap should be close to the canonical value (67), and in order to support a force-free configuration of the magnetosphere a current adjustment mechanism is necessary.

For a current adjustment, high particle density in the magnetosphere is required. Indeed, only a small fraction of all particles could be turned back to the NS. There must be enough inflowing particles to adjust the current density in the polar cap, i.e. its number density should be of the order of $\rho_{\rm GJ}/e$. Hence, the particle number density in the magnetosphere must be $\gg \rho_{\rm GJ}/e$. However, almost all the particles in the magnetosphere are produced in the polar cap and outer gap cascades, and a rather complicated coupling between cascade regions and pulsar magnetosphere arises. The weaker the cascades, the fewer particles are produced there, so the smaller deviation from the GJ current density could be supported. Hence, when a pulsar becomes older, the number of particles created in the polar cap and outer gap cascades is smaller and the maximum deviation of the current density from $j_{\rm GJ}$ will be smaller. If the magnetosphere remains force-free, its configuration must be changed in order to adjust to the new allowed current density. However, this new configuration would result in different energy losses of the pulsar, i.e. the ratio of the real losses to the losses given by the magnetodipolar formula will be different from the same ratio in a previous configuration. So, generally speaking, the evolution of pulsar angular velocity derivative will not follow the power law $\dot{\Omega} \propto -\Omega^3$, as is predicted by the magnetodipolar formula.

In the case of non-stationary cascades there is evidence that no particle inflow into the cascade region may be necessary in order to support current densities both larger and smaller than $j_{\rm GJ}$ (see Levinson et al. 2005). However, for the creation of the 'wave-like' pattern of accelerating electric field (Levinson et al. 2005), necessary for the support of small current densities together with a reasonable pair creation rate, high pair density is required. With the ageing of the pulsar the maximum achieved electric field and pair density will decrease and shorten the range of allowed current densities. This would lead to the evolution of the magnetosphere similar to the case with stationary cascades.

The arguments presented here are based on qualitative analysis of the polar cap cascade properties. In order to make quantitative predictions, a more detailed investigation of polar cap cascades is necessary regarding stationarity, ranges of current densities supported without particle inflow from the magnetosphere, and stability of the cascades in the presence of particle inflow from the magnetosphere.

5.2 Configurations with a Y null point

Let us analyse the behaviour of the magnetosphere of an aligned pulsar under the assumption that the null point is always of a Y type. Here again we mean this in a time-average sense, i.e. we neglect possible non-stationary processes (see e.g. Komissarov 2006; Contopoulos 2005) in the current sheet operating on small scales ($\ll R_{\rm LC}$), such as the building of small plasmoids. If non-stationary variations of the current sheet remains small, the stationary solution should adequately describe the properties of the magnetosphere. The total energy of the magnetosphere decreases with increasing x_0 (see Fig. 10). Apparently the system will try to achieve the configuration with the minimum possible energy, when $x_0 = 1$. However, when the restrictions set by the polar cap cascades are taken into account the picture becomes more complicated.

In solutions with a Y null point the current density in the magnetosphere close to the polar cap boundaries is always less than the GJ current density; it does not exceed the Michel current density (see Section 4.1, Fig. 5). The current adjustment mechanism could adjust the current density to values of *less* than $j_{\rm GJ}$ for the stationary cascade model with no particle escape from the NS surface, in the Ruderman & Sutherland (1975) model. If the pulsar operates in SCLF regime the current density cannot be essentially less than $j_{\rm GJ}$. Hence, force-free solutions with a Y null point are possible if the stationary polar cap cascade operates in a Ruderman–Sutherland regime, or if the cascade is significantly non-stationary; the latter case, however, demands more detailed investigations. On the other hand, for the solutions with $x_0 \gtrsim 0.6$, the current density $j_{\rm pc}$ close to the polar cap boundary has a different sign than $j_{\rm GJ}$ and such force-free configurations are probably never realized.

As was mentioned in Section 5.1, the inflowing particles could be produced either in the pulsar wind or in the outer gap cascades. The outer gap cascade could operate at the surface where GJ charge density changes sign (Cheng et al. 1976). Only a relatively small amount of open field lines cross this surface. Hence, particles produced in the outer gap cascades could not adjust the current density along all magnetic field lines. In Fig. 12 we plot the current density in the polar cap of the pulsar for several x_0 and indicate by the dashed line the colatitudes where particle inflow from the outer gap cascade would be possible. The critical colatitude, where particle inflow from the outer gap cascade is still possible, corresponds to the field line with the smallest ψ passing the surface of $\rho_{\rm GJ} = 0$ inside the LC. At other colatitudes, reversed particles from the pulsar wind (from inside the LC!) are necessary in order to adjust the current density.

In Fig. 5 one can see that the deviation of the current density from $j_{\rm GJ}$, although remaining large, becomes smaller with decreasing x_0.

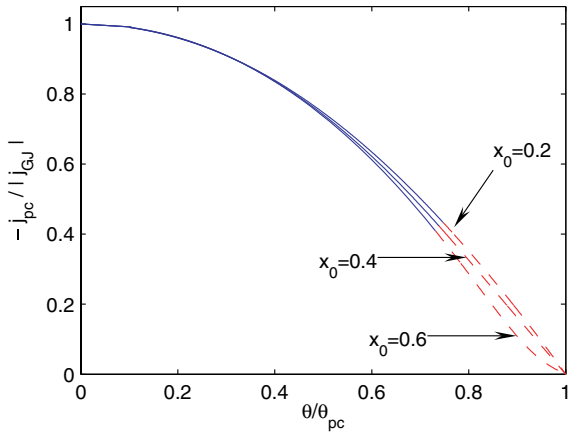

Figure 12. Current density distribution in the polar cap of pulsar $j_{\rm pc}$ as a function of the colatitude. Normalization of physical quantities is the same as in Fig. 5. The colatitude ranges where the current density deviation from $j_{\rm GJ}$ could be supported by particles produced in outer gap cascades are indicated by dashed lines. The current density at colatitudes where $j_{\rm pc}$ is shown by solid line should be supported by particles *reversed* inside the LC.

Thus, if the magnetosphere remains force-free, with the ageing of the pulsar the configuration should change to the one with a smaller current density deviation from $j_{\rm GJ}$. Hence, if the force-free magnetosphere preserves its topology, with the slow-down of the neutron star the size of the closed field line zone becomes smaller. The immediate consequence of this is an increase of the electromagnetic energy losses to the corresponding 'magnetodipolar' energy losses according to equation (62) (see Fig. 8). Let us approximate the dependence of x_0 on the angular velocity of NS rotation by the power law

$$x_0 \propto \Omega^{\xi}\,, \tag{68}$$

where ξ is in reality a (complicated) function of pulsar age. $\xi > 0$ because x_0 decreases as the pulsar gets older. Substituting this into the formula for pulsar energy losses (62) we get

$$W \propto \Omega^{\alpha}, \qquad \alpha = 4 - 2.065\,\xi\,, \tag{69}$$

and for a pulsar braking index

$$n = \frac{\ddot{\Omega}\Omega}{\dot{\Omega}^2} = \alpha - 1 = 3 - 2.065\,\xi\,, \tag{70}$$

i.e. the breaking index is always less than 3!

Let us speculate that configurations with a Y null point are energetically preferable over all possible solutions (force-free and non-force-free ones) and the polar cap cascade operates in the Ruderman–Sutherland regime. Then, as long as particles produced in the cascade regions will be able to support necessary current densities, the pulsar magnetosphere should evolve with time as described above, and at each moment of time the configuration should be stable. Indeed, due to the reconnection of open field lines in the equatorial current sheet the magnetosphere tries to achieve the energetically most preferably configuration, with $x_0 = 1$, but weaker cascades could not inject enough particles into the magnetosphere and support a larger deviation of the current density from $j_{\rm GJ}$. Therefore, x_0 at each moment of time corresponds to the configuration with the current distribution having the maximum possible deviation from $j_{\rm GJ}$. The polar cap cascade zone is *the part* of the whole system which does not allow the closed field zone to have the maximum possible size. The conclusions of Spitkovsky (2005), Komissarov (2006) and McKinney (2006), about instability of all configurations with $x_0 < 1$, is the result of an assumption about the possibility of an arbitrary current density distribution in the pulsar magnetosphere.

We should note also another peculiarity in the Y-configuration– the jump in the surface charge density along the separatrix in the null point, where the charge density changes sign (see Section 4.3 and Fig. 6). The return current flows along the separatrix: electrons to the NS, ions/positrons from the NS. The surface charge density in the current sheet has different sign before and after the null point. We note that there is a jump in the charge density, not just a continuous changing of the charge density such as takes place across the surface where $\rho_{\rm GJ} = 0$. What happens in the null point that such a jump in the charge density could be supported when there is a continuous particle flow carrying the return current? Does an electron–positron cascade operates here? Both the magnetic field and soft X-ray radiation of the NS are too weak here and electron–positron pair creation is suppressed. This problem requires additional investigation.

5.3 Alternatives to force-free Y configurations

In the force-free magnetosphere with a Y-like null point the deviation of the current density from $j_{\rm GJ}$ is always large $> |j_{\rm GJ} - j_{\rm Michel}|$, especially close to the polar cap boundaries. For an older pulsar with weak cascades it would be problematic to adjust the current flowing through the polar cap to the required value. On the other hand, even if force-free Y-configurations are energetically more preferable over the whole class of possible solutions, the stationary polar cap cascade operating in SCLF regime does not allow the current density necessary to support a Y-configuration even in young pulsars. In those cases, the magnetosphere could become non-force-free.

The possible alternative to a magnetosphere becoming non-force-free at a distance of the order of $R_{\rm LC}$ from the NS would be a force-free magnetosphere with an X-like null point. The current density deviation from the GJ current density in the magnetosphere with an X-like null point would be less than that in the Y-configuration for the following reason. In the X-configuration with $x_0 < 1$, condition (39) must be satisfied in points at the LC above A and below A' (see Fig. 13). In those points $\partial_x \psi > 0$, consequently $SS'(\psi \leqslant \psi_{\rm last}) > 0$ and $j(\psi \leqslant \psi_{\rm last}) < 0$ everywhere, neither changing sign nor approaching zero. In principle, for x_0 not to close to the LC and points A, A' not too close to the equatorial plane, the deviation of the current density from $j_{\rm GJ}$ could be made rather small, allowing even weak cascades to support the current density, because in this case only a small correction to the current density would be necessary. It is not clear yet if force-free X-configurations exist or what they would look like (this work is in progress), however there is no clear physical reason forbidding such a possibility.

For an X-configuration, the jump in the surface charge density of the current sheet in the null point could be avoided or at least reduced in magnitude. Considerations from Section 4.3 can be applied to the current sheet separating regions [2(2′)] and [3] in Fig. 13. If the directions of the poloidal magnetic field in these regions coincide,[7] the charge density in this current sheet could be negative too. Indeed, the electric field in regions [2] (E_2) and [3] (E_3) close to the separatrix in that case has the same direction. If $E_3 > E_2$, the charge density of the current sheet is negative and for such configuration the charge density at the separatrix does not change sign, but even if $E_2 > E_3$ the positive charge density would be less than in the case of an equatorial current sheet, when the electric field has to change sign. If the directions of the poloidal magnetic field in these regions are different, the same problem with the current sheet as in the Y-configuration arises for any values of the electric field inside region [3].

The X-configuration was criticized (Lyubarskii 1990) because in the force-free case there is no source of external magnetic field, which could fill region [3] in Fig. 13. However, once formed, this region may be supported by the global current system in the magnetosphere. Reconnection in the equatorial current sheet (Komissarov 2006; Contopoulos 2005) could lead to instantaneous formation of magnetic loops, which would grow in size and form some kind of X-configuration. These loops would try to merge with the closed field line zone or fly away, but the current distribution in the force-free magnetosphere will not support such configurations, so the resulting X-configuration could be stable. What force-free solutions with an X null point would look like is not clear at the moment; maybe there could be solutions with many X null points, i.e. when there are several islands of closed field lines along the equatorial plane (see Fig. 13b), but such complicated systems may be unstable. On the other hand, the configuration shown in

[7] The current sheet in such a configuration is necessary, because in the force-free magnetosphere charged particles cannot flow across magnetic field lines, so after the null point they should flow along a very thin layer too.

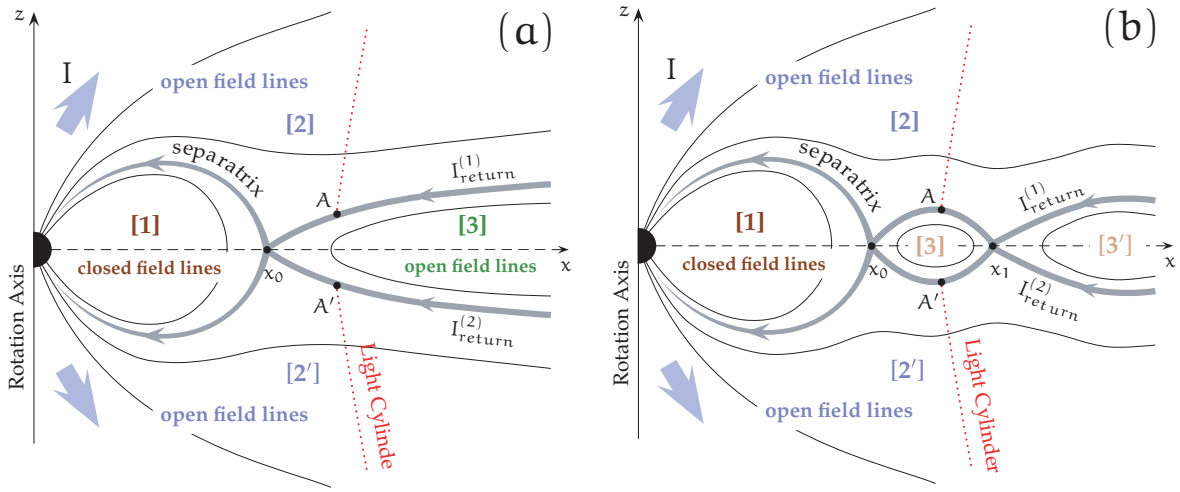

Figure 13. Configurations of magnetic field in the magnetosphere of an aligned rotator with X-null point. (a) – After the null point x_0 the separatrix goes away from the equatorial plane but then intersects it. There are three regions with open magnetic field lines: [2], [2′] and [3]. (b) – After the null point x_0 the separatrix goes away from the equatorial plane but than intersects it (several) times in points $x_1, \ldots$. There are several regions with closed magnetic field lines: [1], [3] and [3′].

Fig. 13(a)[8] cannot be entirely force-free. Indeed, there is no poloidal current in region [3], as it has to have the same direction in both hemispheres, hence the magnetic field there is purely poloidal. This implies that the plasma here does not rotate and there are no currents in the force-free case that could generate the magnetic field. However, we could speculate that in region [3] at some (large) distance from the null point, where the force-free approximation is broken, a system of currents is built up, which also generate the magnetic field in the force-free domain of region [3], close to the null point. In this case the magnetosphere may be force-free at several sizes of the LC.

Time-dependent simulations of an aligned rotator magnetosphere probably could clarify the kind of configuration that is realized. The simulations of Spitkovsky (2005), Komissarov (2006) and McKinney (2006) do not incorporate restrictions on the electric current in the magnetosphere due to polar cap cascade. In time-dependent codes, the restriction set by the polar cap cascades should be formulated in the form of boundary conditions on the poloidal current density. This could be achieved, for example, by the introduction of an artificial Ohm's law along open field lines in the 'polar cap' of the pulsar, i.e. in regions close to the NS surface, such as

$$\boldsymbol{j} = \max(\sigma_{||}\boldsymbol{E},\ \boldsymbol{j}_{\rm cas})\,, \qquad (71)$$

where $\boldsymbol{j}_{\rm cas}$ corresponds to the minimal possible current density along the particular field line allowed by cascades. $\sigma_{||}$ is the conductivity along the magnetic field lines, specific to each particular code. In order to set these restrictions, the knowledge of the polar cap cascade properties is necessary, which is another very complicated problem.

The possibility of a non-stationary magnetosphere also cannot be excluded at the current stage of research. In order to decide between possible configurations (e.g. force-free with X or Y null points, non-force-free stationary magnetosphere or significantly non-stationary configurations) more detailed studies of polar cap cascades and the stability of the current sheet are necessary .

[8] Such a configuration has been considered in several works (e.g. Beskin et al. 1993; Beskin & Malyshkin 1998).

6 CONCLUSIONS

We have studied in detail stationary configurations of the force-free magnetosphere of an aligned rotator with a Y null point. This assumption about the Y-configuration of the magnetosphere is very popular and this case had demanded careful investigation. We find a set of force-free solutions parametrized by the position of the neutral point x_0. Results presented in this work for $x_0 = 1$ agree very well with ones obtained by other authors (Contopoulos 2005; Gruzinov 2005; Komissarov 2006; Spitkovsky 2005). We calculated the physical characteristic of obtained solutions and analysed properties of force-free magnetosphere with a Y-like null point. For solutions with x_0 close to 1 we found that, despite similarly distributed magnetic surfaces at large distances from the LC, they differ substantially from the split monopole solution of Michel (1973b) regarding the distribution of physical quantities (drift velocity, energy flux distribution, etc.). When the null point lies well inside the LC, solutions approach the Michel one, the agreement being better for smaller values of x_0.

We analysed the role that cascades in the polar cap play in the formation of the overall structure of the magnetosphere. Although its properties depend mostly on the local physics in the polar cap of pulsar, this cascade region sets serious limitations on the current density in the whole magnetosphere. In some sense the non-trivial physics of the cascades plays the role of complicated boundary conditions for MHD equations that describe the structure of the magnetosphere – arbitrary current density is not allowed. Changes in boundary conditions influence the whole solution. We argue that not all possible Y-configurations can be realized. Moreover, the restrictions set by some cascade models questions the existence of a stationary force-free Y-configuration. In our opinion, there are two problems with the force-free magnetosphere in the Y-configuration: (i) the current density strongly deviates from the GJ current density, and (ii) the charge density along the current sheet has discontinuity and changes sign. These problems could be avoided in stationary force-free X-configurations.

We argue that with the ageing of pulsar and decreasing of the cascade power, the magnetosphere must evolve with time, i.e. it

should change to the configurations where the deviation of the current density from $j_{\rm GJ}$ will be smaller. In the case of a force-free Y-configuration the closed field line zone grows more slowly than the LC during pulsar slowdown. This leads to a *decreasing* pulsar breaking index below the value 3, predicted by the magnetodipolar formula. This effect is present in the aligned rotator because of the current adjustment in the polar cap of the pulsar. Similar behaviour should also be present in configurations with an X-like null point. In an analytical model of Beskin & Malyshkin (1998) it was shown that the minimum energy of the magnetosphere is achieved when x_0 approaches the LC. Although their model is an oversimplification of the real problem, this result should be qualitatively true. An X-configuration with $x_0 = 1$ requires strong deviations of j from $j_{\rm GJ}$, so as the pulsar ages, x_0 should decrease, increasing the number of open field lines, leading to increased energy losses and a decreased pulsar breaking index. This should also be true for an inclined rotator, at least for not very large inclination angles. Recently, Contopoulos & Spitkovsky (2006) proposed another explanation for the breaking index of a pulsar being less than 3. In their model it is caused also by a shrinking of the closed field line zone, but they assumed this is due to differences in the characteristic time, at which the magnetosphere reaches the new configuration due to the reconnection of new magnetic field lines, and the time of increase of the LC radius. However, the reason of such a slow reconnection in the current sheet is not clear.

The solutions obtained could be used for comparison with observations. For example, magnetic field lines are differently twisted in different solutions; this could be compared with magnetic field geometry inferred from pulsar polarization measurements (see Dyks & Harding 2004, and references therein). However, the real pulsar magnetosphere could be non-stationary and/or non-force-free, and this issue could be verified only within a more detailed time-dependent approach. On the other hand, in the latter case observational manifestations of the pulsar will be significantly different from models with a force-free magnetosphere, where the main emission comes from the polar cap and from the outer gap zones.

ACKNOWLEDGMENTS

I thank V. Beskin for numerous fruitful discussions, helpful suggestions and encouraging comments. I'm grateful to A. Spitkovsky for fruitful discussions and useful comments on the draft version of this article. I acknowledge K. Hirotani, Yu. Lyubarskij, and J. Pétri for discussions. I wish to thank anonymous referee for helpful critical comments. I thank the Max-Planck-Institut für Kernphysik (Heidelberg, Germany) for their hospitality. This work was partially supported by the German Academic Exchange Service (DAAD) grant A/05/05462, and the RFBR grant 04-02-16720.

REFERENCES

Arons J., 1979, Space Sci. Rev., 24, 437
Beskin V. S., 2005, Osesimmetrichnye Stacionarnye Techeniya v Astrofizike. Fizmatlit, Moscow (in Russian)
Beskin V. S., Malyshkin L. M., 1998, MNRAS, 298, 847
Beskin V. S., Gurevich A. V., Istomin I. N., 1983, Zh. Eksp. Teor. Fiz., 85, 401
Beskin V., Gurevich A., Istomin Y., 1993, Physics of the Pulsar Magnetosphere. Cambridge Univ. Press, Cambridge
Beskin V. S., Kuznetsova I. V., Rafikov R. R., 1998, MNRAS, 299, 341
Blandford R. D., 2002, in Gilfanov M., Sunyaev R., Churazov E., eds, Proc. MPA/ESO, Lighthouses of the Universe: the most Luminous Celestial Objects and their Use for Cosmology. ESO, Garching, p. 381
Bogovalov S. V., Chechetkin V. M., Koldoba A. V., Ustyugova G. V., 2005, MNRAS, 358, 705
Cheng A., Ruderman M., Sutherland P., 1976, ApJ, 203, 209
Contopoulos I., 2005, A&A, 442, 579
Contopoulos I., Spitkovsky A., 2006, ApJ, in press (astro-ph/0512002)
Contopoulos I., Kazanas D., Fendt C., 1999, ApJ, 511, 351
Daugherty J. K., Harding A. K., 1982, ApJ, 252, 337
Dyks J., Harding A. K., 2004, ApJ, 614, 869
Goldreich P., Julian W. H., 1969, ApJ, 157, 869
Goodwin S. P., Mestel J., Mestel L., Wright G. A. E., 2004, MNRAS, 349, 213
Gruzinov A., 2005, Phys. Rev. Lett., 94, 021101
Hibschman J. A., Arons J., 2001, ApJ, 554, 624
Ingraham R. L., 1973, ApJ, 186, 625
Komissarov S. S., 2002, MNRAS, 336, 759
Komissarov S. S., 2006, MNRAS, 367, 19
Komissarov S. S., Lyubarsky Y. E., 2003, MNRAS, 344, L93
Levinson A., Melrose D., Judge A., Luo Q., 2005, ApJ, 631, 456
Lyubarskii Y. E., 1990, SvA Lett., 16, 16
Lyubarskij Y. E., 1992, A&A, 261, 544
McKinney J. C., 2006, MNRAS, in press (doi:10.1111/j.1745-3933.2006.00150.x) (astro-ph/0601411)
Mestel L., 1973, Ap&SS, 24, 289
Mestel L., Wang Y.-M., 1979, MNRAS, 188, 799
Michel F. C., 1973a, ApJ, 180, 207
Michel F. C., 1973b, ApJ, 180, L133
Michel F. C., 1991, Theory of Neutron Star Magnetospheres. Univ. of Chicago Press, Chicago, p. 533
Muslimov A. G., Tsygan A. I., 1992, MNRAS, 255, 61
Okamoto I., 1974, MNRAS, 167, 457
Pétri J., Heyvaerts J., Bonazzola S., 2002, A&A, 384, 414
Ruderman M. A., Sutherland P. G., 1975, ApJ, 196, 51
Scharlemann E. T., Wagoner R. V., 1973, ApJ, 182, 951
Scharlemann E. T., Arons J., Fawley W. M., 1978, ApJ, 222, 297
Smith I. A., Michel F. C., Thacker P. D., 2001, MNRAS, 322, 209
Spitkovsky A., 2004, in Camilo F., Gaensler B. M., eds, Proc. IAU Symp., 218, Young Neutron Stars and Their Environments. Astron. Soc. Pac., San Francisco, p. 357
Spitkovsky A., 2005, in Bulik T., Rudak B., Madejski G., eds, Proc. AIP Conf., Vol. 801, Astrophysical Sources of High Energy Particles and Radiation. Am. Inst. Phys., New York, p. 253
Spitkovsky A., Arons J., 2002, in Slane P. O., Gaensler B. M., eds, ASP Conf. Ser., Vol. 271, Neutron Stars in Supernova Remnants. Astron. Soc. Pac., San Francisco, p. 81
Spitkovsky A., Arons J., 2004, ApJ, 603, 669
Sturrock P. A., 1971, ApJ, 164, 529
Sulkanen M. E., Lovelace R. V. E., 1990, ApJ, 350, 732
Takata J., Shibata S., Hirotani K., 2004, MNRAS, 354, 1120
Timokhin A. N., 2005, in Bulik T., Rudak B., Madejski G., eds, Proc. AIP Conf., Vol. 801, Astrophysical Sources of High Energy Particles and Radiation. Am. Inst. Phys., New York, p. 330
Trottenberg U., Oosterlee C. W., Schüller A., Brandt A., Oswald P., Stüben K., 2001, Multigrid. Academic Press, New York
Uzdensky D. A., 2003, ApJ, 598, 446

APPENDIX A: CURRENT DENSITY IN THE POLAR CAP

The poloidal current density is given by (see Beskin 2005)

$$\boldsymbol{j}_{\rm pol} = \frac{\nabla I \times \boldsymbol{e}_\phi}{\varpi} = \frac{{\rm d}I}{{\rm d}\Psi}\boldsymbol{B}_{\rm pol}\,, \tag{A1}$$

the latter expression was obtained by taking into account relation (10). Substituting for $\boldsymbol{B}_{\rm pol}$, the expression for the dipole magnetic

field at the NS surface $\boldsymbol{B}_{\rm pol} = B_0(\boldsymbol{e}_r \cos\theta + (1/2)\,\boldsymbol{e}_\theta \sin\theta)$, and expressing I and Ψ through normalized quantities, we get for the poloidal current density in the polar cap of pulsar

$$j_{\rm pc} = |j_{\rm GJ}|\,\frac{1}{2}S'(\psi)\sqrt{1-\frac{3}{4}\sin^2\theta}\,, \tag{A2}$$

where $|j_{\rm GJ}|$ is the absolute value of the GJ current density in the polar cap

$$|j_{\rm GJ}| = \frac{B_0\Omega}{2\pi c}\,c\,. \tag{A3}$$

For a dipole magnetic field in the polar cap (see equation 44)

$$\psi = \frac{R_{\rm LC}}{R_{\rm NS}}\sin^2\theta \approx \frac{R_{\rm LC}}{R_{\rm NS}}\theta^2\,. \tag{A4}$$

The colatitude of the polar cap boundary is $\theta_{\rm pc} = 1.45\times 10^{-2}P^{-1/2}\sqrt{\psi_{\rm last}}$; P is the period of pulsar in seconds. Thus, $\theta^2 < {\theta_{\rm pc}}^2 \ll 1$ and the term with $\sin^2\theta$ in equation (A2) can be neglected. From equation (A4) we have the relation between the colatitude θ in the polar cap and the corresponding magnetic flux function ψ

$$\psi = \psi_{\rm last}\left(\frac{\theta}{\theta_{\rm pc}}\right)^2\,. \tag{A5}$$

Substituting this relation into equation (A2) we get

$$j_{\rm pc} = |j_{\rm GJ}|\,\frac{1}{2}S'\left[\left(\frac{\theta}{\theta_{\rm pc}}\right)^2\psi_{\rm last}\right]\,. \tag{A6}$$

APPENDIX B: ENERGY LOSSES

The poloidal component of the Poynting flux in the magnetosphere of an aligned rotator is

$$\boldsymbol{P}_{\rm pol} = \frac{c}{4\pi}[\boldsymbol{E}\times\boldsymbol{B}]_{\rm pol} = -\frac{\Omega_{\rm F}}{c}\,I\,\boldsymbol{B}_{\rm pol}\,, \tag{B1}$$

the latter expression was obtained with help of equations (8) and (14). Expressing $\boldsymbol{B}_{\rm pol}$ through Ψ, equation (9), we have for the radial component of the Poynting flux

$$P_r = -\frac{I\Omega_{\rm F}}{c}\frac{1}{\varpi r}\left(Z\,\partial_\varpi\Psi - \varpi\,\partial_Z\Psi\right)\,, \tag{B2}$$

where $r = \sqrt{\varpi^2+Z^2}$. Energy losses per solid angle $\mathrm{d}\omega$ are $\mathrm{d}W = -r^2P_r\,\mathrm{d}\omega$. The angular distribution of energy losses are given by

$$\frac{\mathrm{d}W}{\mathrm{d}\omega} = \frac{I\Omega_{\rm F}}{c}\frac{r}{\varpi}\left(Z\,\partial_\varpi\Psi - \varpi\,\partial_Z\Psi\right)\,. \tag{B3}$$

Using normalized quantities we rewrite this equation as

$$\frac{\mathrm{d}W}{\mathrm{d}\omega} = \frac{|W_{\rm md}|}{4\pi}\,S\frac{\sqrt{x^2+z^2}}{x}\left(z\,\partial_x\psi - x\,\partial_z\psi\right)\,, \tag{B4}$$

where $|W_{\rm md}|$ is the absolute value of the magnetodipolar energy losses, here defined as

$$|W_{\rm md}| \equiv \frac{\mu^2}{R_{\rm LC}^4}c = \frac{B_0^2R_{\rm NS}^6\Omega^4}{4c^3}\,. \tag{B5}$$

Energy losses of an aligned rotator can be obtained by the integration of equation (B3):

$$W = \int_{4\pi}\frac{\mathrm{d}W}{\mathrm{d}\omega}\,\mathrm{d}\omega = 2\int_0^{\Psi_{\rm last}}\frac{2\pi}{c}I\Omega_{\rm F}\,\mathrm{d}\Psi\,; \tag{B6}$$

the factor of 2 appears because energy is carried away by the Poynting flux from both hemispheres. Using the normalized quantities introduced at the end of the Section 2.1, this formula can be rewritten as

$$W = \frac{\mu^2}{R_{\rm LC}^4}c\int_0^{\psi_{\rm last}}S\,\mathrm{d}\psi = |W_{\rm md}|\int_0^{\psi_{\rm last}}S\,\mathrm{d}\psi\,. \tag{B7}$$

An analytical formula for estimation of aligned rotator energy losses could be obtained in the following way. Poloidal current S for each of obtained solutions does not deviate much from Michel's current function, equation (50). Substituting this function into equation (B7), we get

$$W \approx -\frac{2}{3}\psi_{\rm last}^2\,|W_{\rm md}|\,. \tag{B8}$$

We could estimate the dependence of $\psi_{\rm last}$ on x_0 using the magnetic flux function of the dipolar field; equation (19). Substituting $\psi^{\rm dip}(x_0) = x_0^{-1}$ into equation (B8), we get

$$W \approx -\frac{2}{3}x_0^{-2}\,|W_{\rm md}|\,. \tag{B9}$$

APPENDIX C: THE SIZE OF THE REGION WHERE PARTICLE INFLOW IS POSSIBLE

Charged particles in crossed electric and magnetic fields drift with the velocity $\boldsymbol{U}_{\rm D}$ given by equation (16), which can be rewritten as

$$\boldsymbol{U}_{\rm D} = \frac{\Omega_{\rm F}\varpi}{B^2}\left({B_{\rm pol}}^2\boldsymbol{e}_\phi - B_\phi\boldsymbol{B}_{\rm pol}\right). \tag{C1}$$

In general, a charged particle in the magnetosphere could have two velocity components: one perpendicular to the magnetic field line (the drift velocity) and an additional component along the magnetic field line, $U_{||}$ (see Fig. C1). With increasing distance from the NS, $U_{\rm D}$ increases (see Fig. 3). The velocity of the particle U can not exceed the speed of light, hence the parallel component of particle velocity far from the NS must be also smaller. The magnetic field lines far from the NS are strongly twisted and at some distance the particle radial velocity component will be positive, i.e. directed from the NS, for any direction of the parallel component. At these distances, particles can flow only *from* the NS. Let us show that the

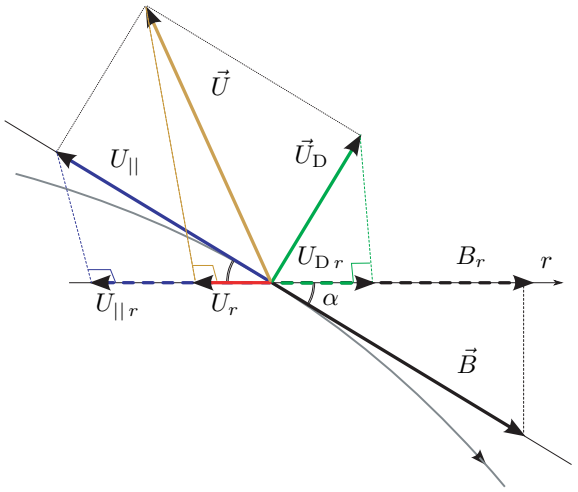

Figure C1. Particle velocity decomposition in $U_{||}$ and $U_{\rm D}$. The mgnetic field line is shown by the thick curved line.

size of the domain where particles could flow to the NS corresponds to the size of the LC.

From Fig. C1 it is evident that the radial component of the total particle velocity is

$$U_r = U_{\mathrm{D}r} + U_{||r}\,. \tag{C2}$$

The maximum value of the velocity component parallel to the magnetic field is

$$U_{||}^{\max} \simeq \sqrt{c^2 - \boldsymbol{U}_{\mathrm{D}}^2}\,. \tag{C3}$$

If the radial component of the magnetic field $B_r > 0$, then for the azimuthal component of the magnetic field $B_\phi = -|B_\phi|$. For radial components of particle velocities we have

$$U_{||r}^{\max} = -\frac{B_r}{B} U_{||}^{\max} \simeq -\frac{B_r}{B} c \sqrt{1 - \left(\frac{\Omega_{\mathrm{F}}\varpi}{c}\right)^2 \frac{{B_{\mathrm{pol}}}^2}{B^2}}, \tag{C4}$$

$$U_{\mathrm{D}r} = \frac{\Omega_{\mathrm{F}}\varpi}{B^2} |B_\phi| B_r. \tag{C5}$$

From this, the maximum possible velocity component in the radial direction is

$$U_r^{\max} \simeq -\frac{B_r}{B} c \left(\sqrt{1 - \left[\frac{\Omega_{\mathrm{F}}\varpi}{c}\right]^2 \frac{{B_{\mathrm{pol}}}^2}{B^2}} - \frac{\Omega_{\mathrm{F}}\varpi}{c} \frac{|B_\phi|}{B} \right) \tag{C6}$$

Particles could flow to the NS only if $U_r^{\max} < 0$, and this is possible if

$$\sqrt{1 - \left(\frac{\Omega_{\mathrm{F}}\varpi}{c}\right) \frac{{B_{\mathrm{pol}}}^2}{B^2}} > \frac{\Omega_{\mathrm{F}}\varpi}{c} \frac{|B_\phi|}{B} \tag{C7}$$

or

$$\varpi < \frac{c}{\Omega_{\mathrm{F}}}\,, \tag{C8}$$

i.e. only inside the LC. For $B_r < 0$ we get the same result. The same restriction, namely that particles could cross the Alfvénic surface (LC in our case) only in one direction, is proved to be valid in the full MHD case too (see e.g. Beskin 2005).

This paper has been typeset from a TEX/LATEX file prepared by the author.